

Chiral Spin Glasses, Chaos, and Spin-Glass Lower-Critical Dimension from Continuously Variable Dimensional Realizations

**Nihat Berker (Kadir Has University, MIT)
Bora Atalay (KHU), Tolga Çağlar (SU),
Efe İlker (SU), Mehmet Demirtaş (SU), Aslı Tuncer (İTÜ)**

**Hierarchical Lattices: Exactly Soluble Systems,
Continuously Variable Spatial Dimension d**

**Spin-Glass Phase Lower-Critical Dimension
And Robust Chaos**

**Chiral Spin Glass Phase and Fibrous Boundaries
Microreentrances**

**Continuum of Devil's Staircases
Deep Reentrance and Inverted Devil's Staircase**

**Multiple (4) Spin-Glass Phases in Same Phase Diagram,
Phase Transitions between Different Spin-Glass Phases
Chaos-to-Chaos Phase Transitions**

Hollywood goes to Statistical Mechanics

New Order in the presence of Frozen Disorder Spin-Glass Systems

"Ordinary" Magnets

$$\mathcal{H} = -J \sum_{\langle ij \rangle} s_i s_j, \quad s_i = \pm 1$$

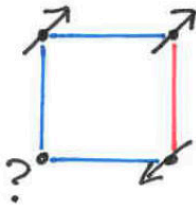
$J > 0$ Ferromagnetic alignment $\uparrow\uparrow\uparrow\uparrow$

$J < 0$ Antiferromagnetic alignment $\uparrow\downarrow\uparrow\downarrow$

Spin Glasses

$$\mathcal{H} = -\sum_{\langle ij \rangle} J_{ij} s_i s_j$$

$J_{ij} = +|J|$ or $-|J|$, frozen randomly



Frustration

New frustration:
From competing L/R
CHIRALITY
(HELICITY).
Chiral Spin-Glass
Phase
and 3 other
new SG phases

Beyin Bilimi ve Nöroloji: Geleceğin Bilimi
Prof. Dr. Sondan Durukanoğlu Feyiz
Kadir Has Üniversitesi Rektör V.

Dersler: Salı günleri 20:00-21:30, 16 Ekim 2018 – 27 Kasım 2018
Olası telafi dersler: 4 - 18 Aralık 2018

İlk ders: Salı 16 Ekim 2018


Ders ve okumalar Türkçe olacaktır.

bilgi için: nihatberker@khas.edu.tr
0532-310-0554

Beynimiz ne kadar karmaşık ve işleyiş mekanizmalarını nasıl anlayabiliriz? Beyin hücrelerimiz etrafını nasıl algılar? Bilgi nöronlar arasında nasıl iletilir? Aksiyon potansiyeli nedir? Nöron hücre zarının basit devre ile matematiksel modellenmesi mümkün mü? Nöronlar birlikte nasıl çalışır (Nöral ağ ve bağlantılar)? Beyindeki aktiviteler nasıl ölçülebilir ve veri nasıl analiz edilir? Beynimiz bir bütün olarak nasıl çalışır ve bilişsel bilim nedir? Bütün bu sorulara birlikte merak ve keyifle yanıt arayacağız.

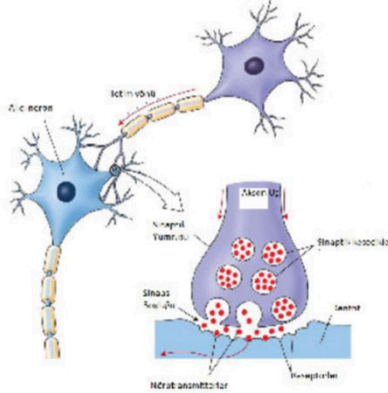
Ders, herkese açıktır. Ders ve okumalar Türkçe olacaktır. Derse katılım için <http://acik-ders.khas.edu.tr> adresine başvurulmalıdır. Derse kabul edilip kayıt olanlar için, kabulden hemen sonra yatırılması gereken geri verilmez 500 TL kayıt ücreti vardır. Dersin kontenjanının çok çabuk dolması beklenmektedir. Ders süresince kısa sınavlar ve dönem sonu sınavı olacaktır. Nota katkıları: Kısa sınavlar 50%, dönem sonu sınavı 50%. Başarılı katılımcılara Üstün Başarı Sertifikası veya Başarı Sertifikası verilecektir.

Beyin | 16.02.2018



BEYİN

Nöronlar birbirleriyle nasıl konuşur?



Bilgi bir nörondan öteki nörona elektrik ve kimya prensiplerine dayalı bir şekilde iletilir

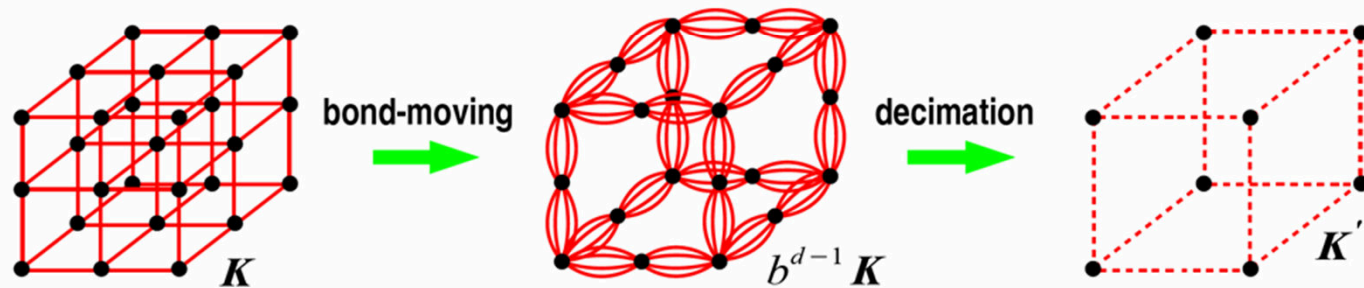
Nöronlar sinaps denilen bağlantı noktaları aracılığı ile birbirleri ile iletişimi sağlar

Sinaps: sinir kavşağı, kimyasal paketçikleri ya da elektrik sinyalleri alır

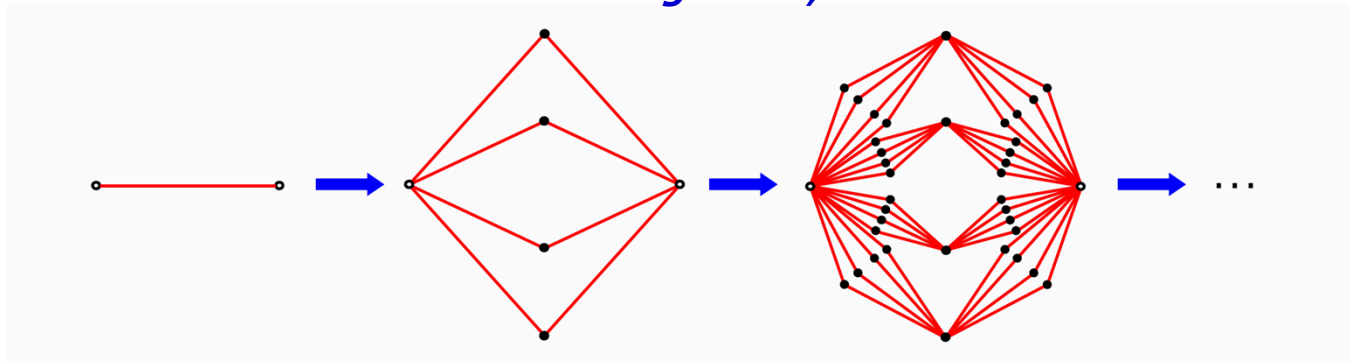
- Aksiyon Potansiyeli (Elektrik)
- Nörotransmitter (kimyasal "paket" ler)

Migdal-Kadanoff procedure for d dimensional hypercubic lattice, with length rescaling factor b :

Example with $d = 3, b = 2$



Equivalent exact model
Construction of a Hierarchical Lattice (d=3)
Length rescaling factor, $b = 2$
Volume rescaling factor, $b^d = 8$



Systems with Quenched Random Interactions
Renormalization of
the Quenched Probability Distribution

$$P'(\mathbf{K}'_{i'j'}) = \int \left(\prod_{ij}^{i'j'} d\mathbf{K}_{ij} P(\mathbf{K}_{ij}) \right) \delta(\mathbf{K}'_{i'j'} - \mathbf{R}(\{\mathbf{K}_{ij}\}))$$

local RG
recursion
relation

Lower lower-critical spin-glass dimension from quenched mixed-spatial-dimensional spin glasses

Bora Atalay¹ and A. Nihat Berker^{2,3}

¹*Faculty of Engineering and Natural Sciences, Sabancı University, Tuzla, Istanbul 34956, Turkey*

²*Faculty of Engineering and Natural Sciences, Kadir Has University, Cibali, Istanbul 34083, Turkey*

³*Department of Physics, Massachusetts Institute of Technology, Cambridge, Massachusetts 02139, USA*



(Received 16 August 2018; published 15 October 2018)

By quenched-randomly mixing local units of different spatial dimensionalities, we have studied Ising spin-glass systems on hierarchical lattices continuously in dimensionalities $1 \leq d \leq 3$. The global phase diagram in temperature, antiferromagnetic bond concentration, and spatial dimensionality is calculated. We find that, as dimension is lowered, the spin-glass phase disappears to zero temperature at the lower-critical dimension $d_c = 2.431$. Our system being a physically realizable system, this sets an upper limit to the lower-critical dimension in general for the Ising spin-glass phase. As dimension is lowered towards d_c , the spin-glass critical temperature continuously goes to zero, but the spin-glass chaos fully subsists to the brink of the disappearance of the spin-glass phase. The Lyapunov exponent, measuring the strength of chaos, is thus largely unaffected by the approach to d_c and shows a discontinuity to zero at d_c .

DOI: [10.1103/PhysRevE.98.042125](https://doi.org/10.1103/PhysRevE.98.042125)

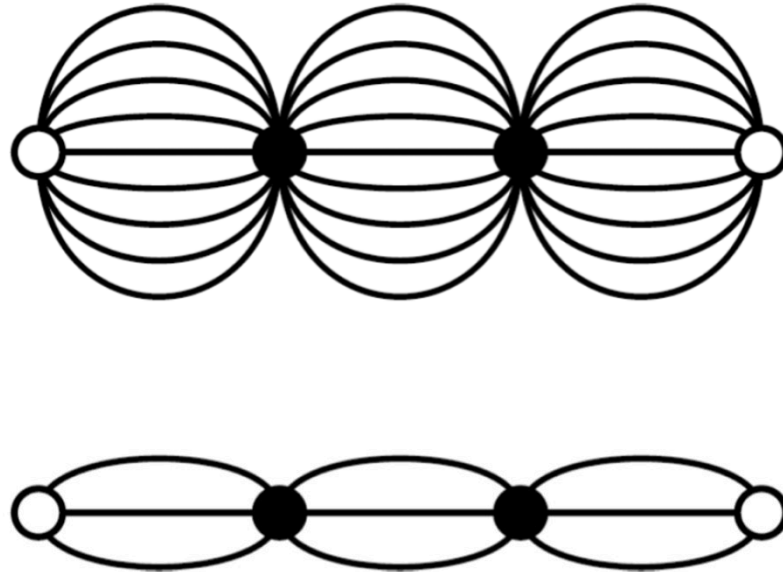
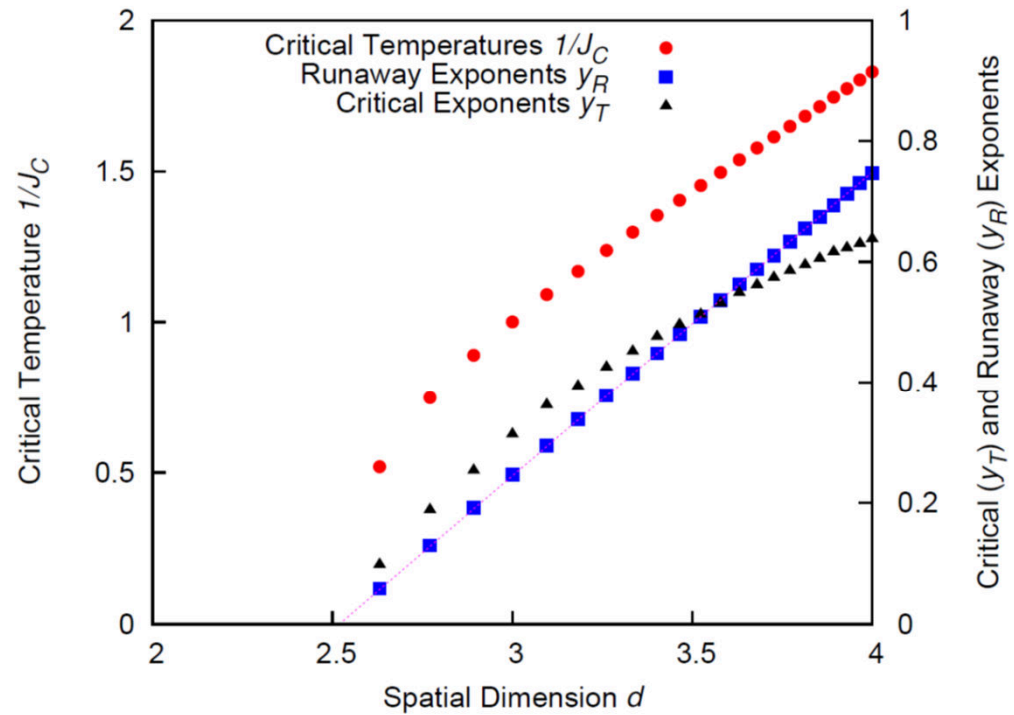
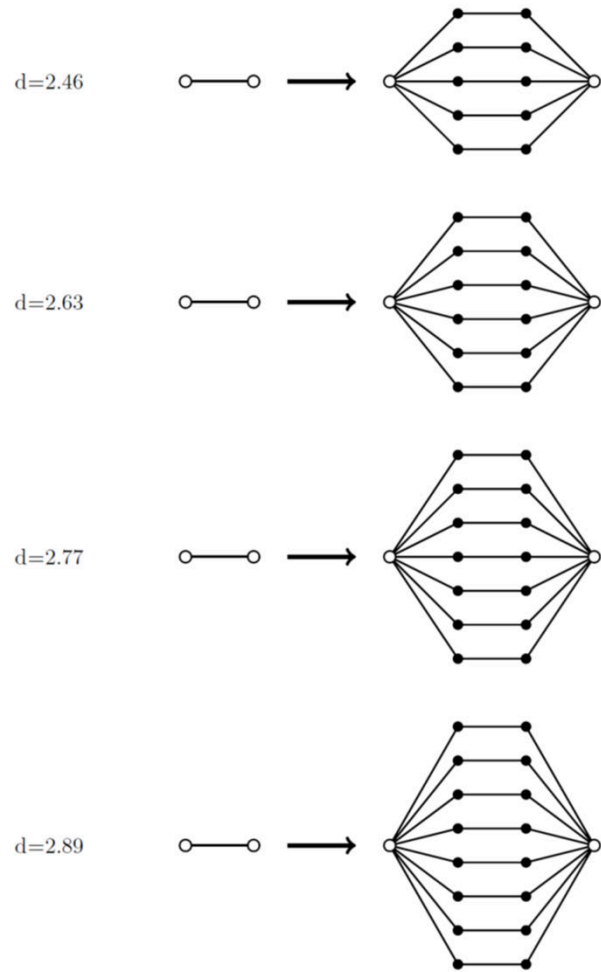


FIG. 1. Local graphs with $d = 2$ (bottom) and $d = 3$ (top) connectivity. The cross-dimensional hierarchical lattice is obtained by repeatedly imbedding the graphs in place of bonds, randomly with probability $1 - q$ and q for the $d = 2$ and $d = 3$ units, respectively.



$$y_R = -1.30908 + 0.528513d - 0.00354805d^2$$

$$R^2 = 0.999999$$

Lower-critical dimension $d_L = 2.520$ =63/25

Mehmet Demirtaş, et al. (2015)

(Linear fit: $R^2 = 0.999992$ $d_L = 2.516$)

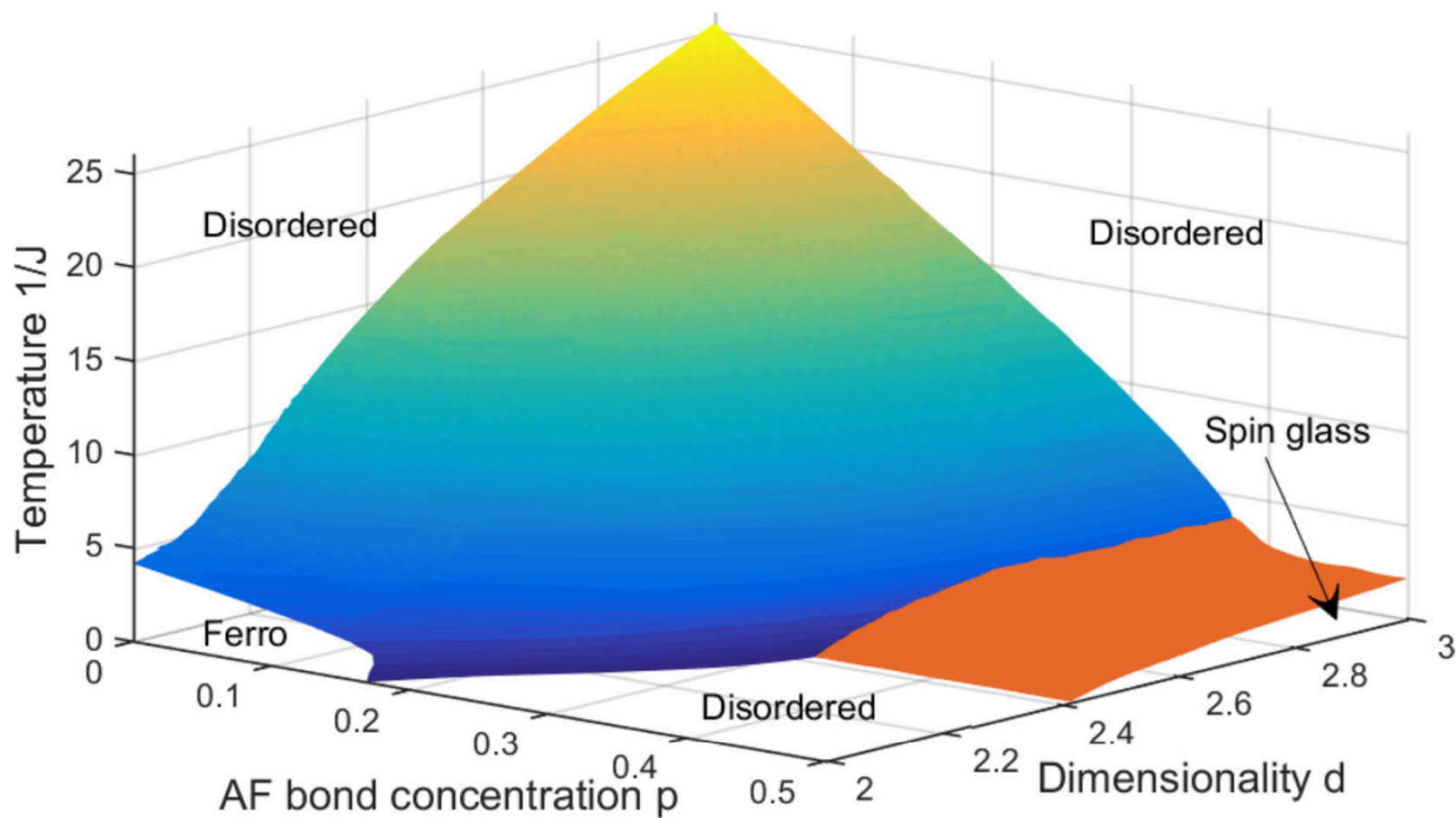


FIG. 2. Calculated exact global phase diagram of the Ising spin glass on the cross-dimensional hierarchical lattice, in temperature $1/J$, antiferromagnetic bond concentration p , and spatial dimension d . The global phase diagram is symmetric about $p = 0.5$; the mirror image portion of $0.5 < p < 1$ is not shown. The spin-glass phase is thus clearly seen, taking off from zero temperature at $d_c = 2.431$.

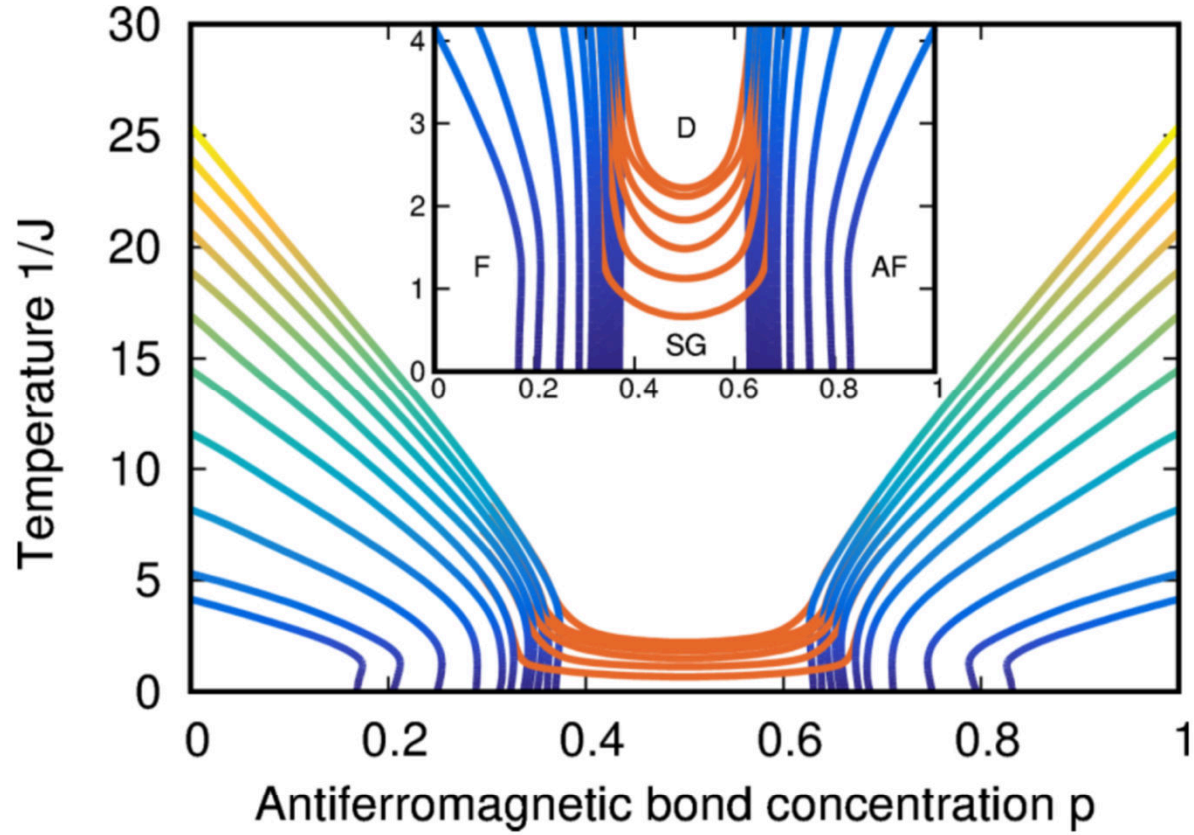


FIG. 3. Constant dimensionality d cross sections of the global phase diagram in Fig. 2. The cross sections are, starting from high temperature, for $d = 3, 2.9, 2.8, 2.7, \dots, 2.1, 2$. It can be seen that, as the dimensionality d approaches $d_c = 2.431$ from above, the spin-glass phase disappears at zero temperature.

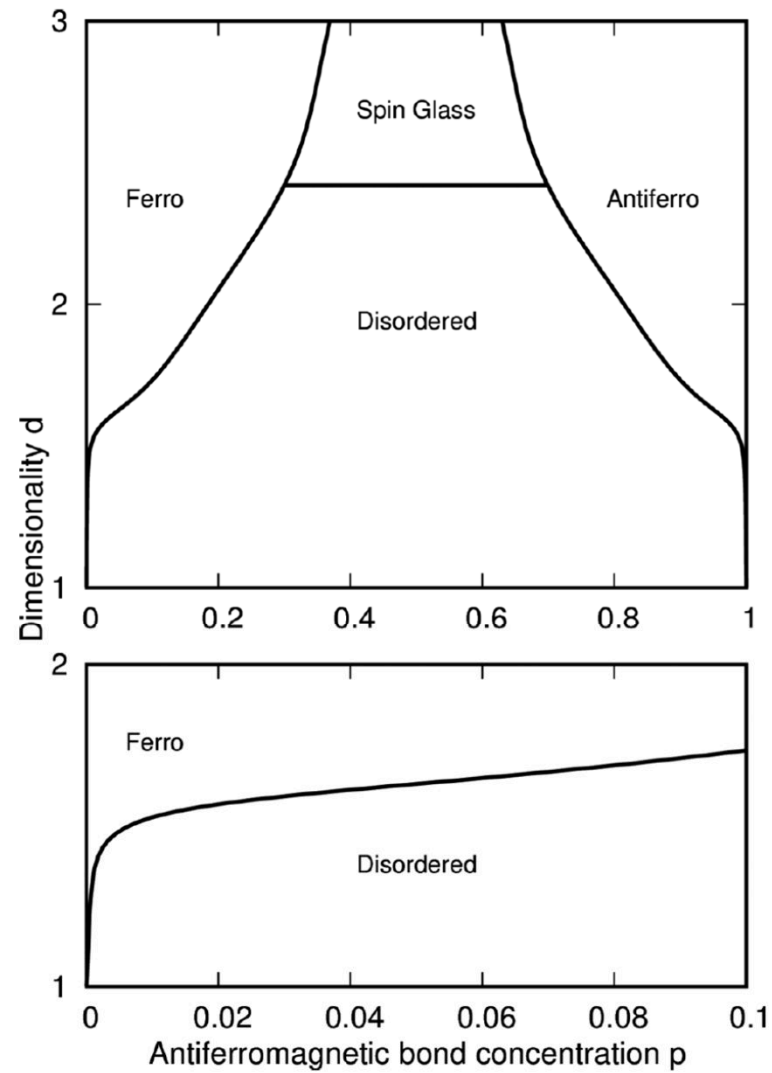
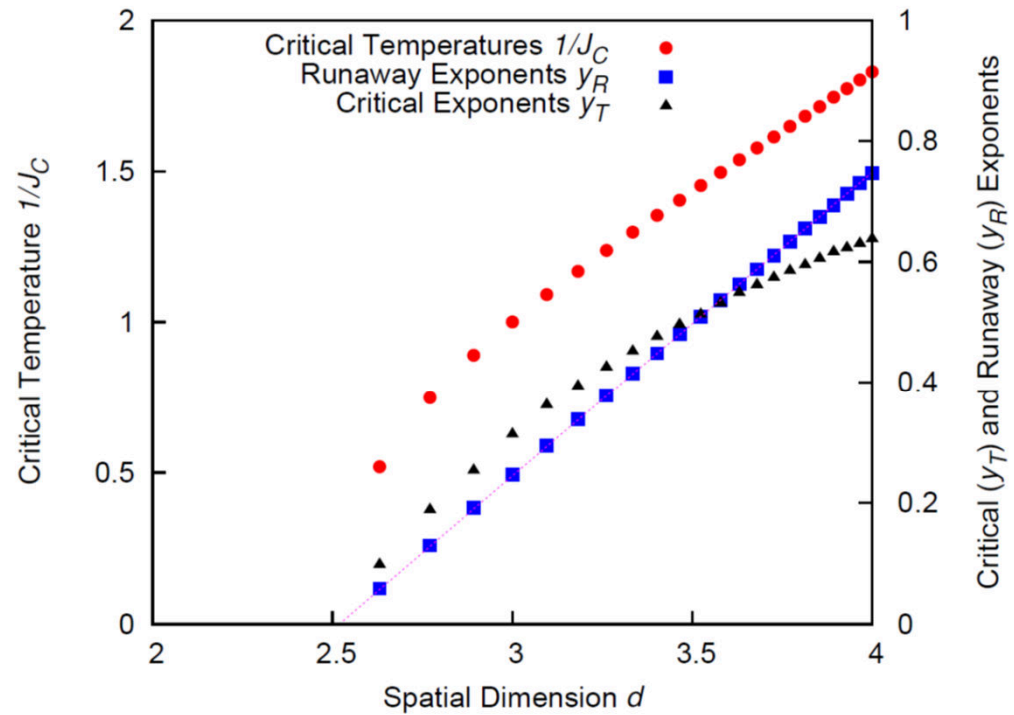
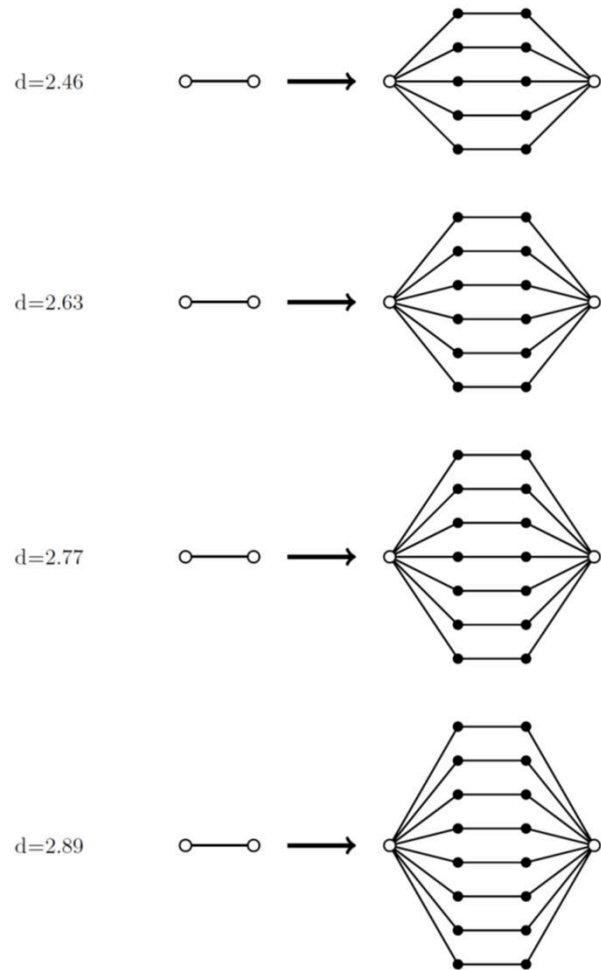


FIG. 4. Zero-temperature phase diagram of the Ising spin-glass system on the cross-dimensional hierarchical lattice, in antiferromagnetic bond concentration p and spatial dimension d . The lower-critical dimension of $d_c = 2.431$ is clearly visible.



$$y_R = -1.30908 + 0.528513d - 0.00354805d^2$$

$$R^2 = 0.999999$$

Lower-critical dimension $d_L = 2.520$ =63/25

Mehmet Demirtaş, et al. (2015)

(Linear fit: $R^2 = 0.999992$ $d_L = 2.516$)

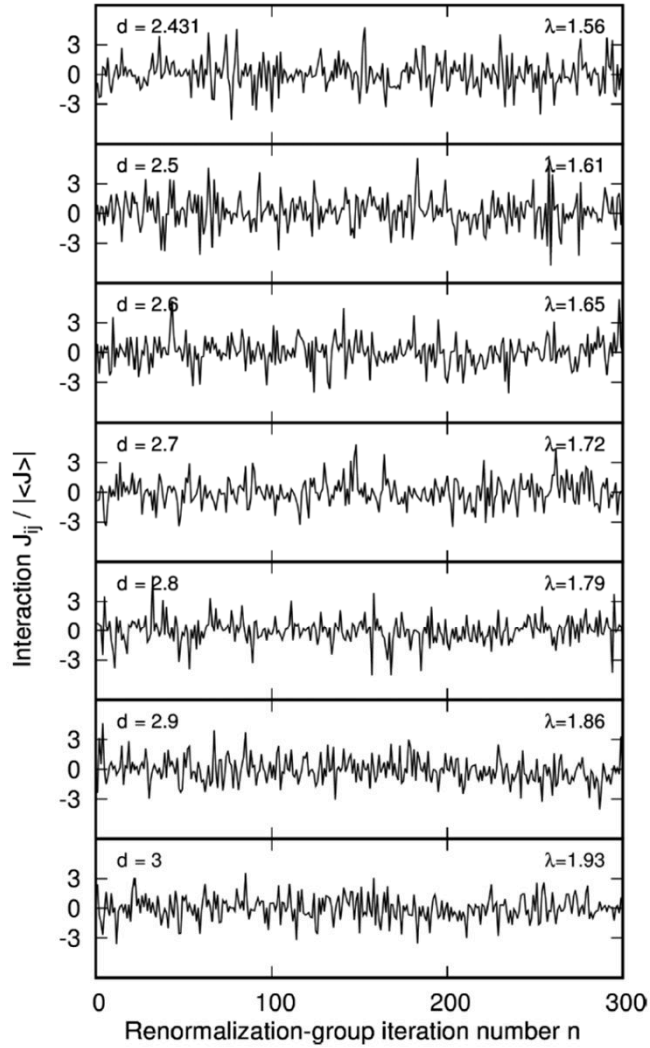


FIG. 5. Chaotic renormalization-group trajectory of the interaction J_{ij} at a given location (ij) , for various spatial dimensions between the lower-critical dimension $d_c = 2.431$ and $d = 3$. Note that strong chaotic behavior, as reflected by the shown calculated Lyapunov exponents λ , nevertheless continues as the spin-glass phase disappears at the lower-critical dimension d_c , as seen in Fig. 6.

$$\lambda = \lim_{n \rightarrow \infty} \frac{1}{n} \sum_{k=0}^{n-1} \ln \left| \frac{dx_{k+1}}{dx_k} \right|$$

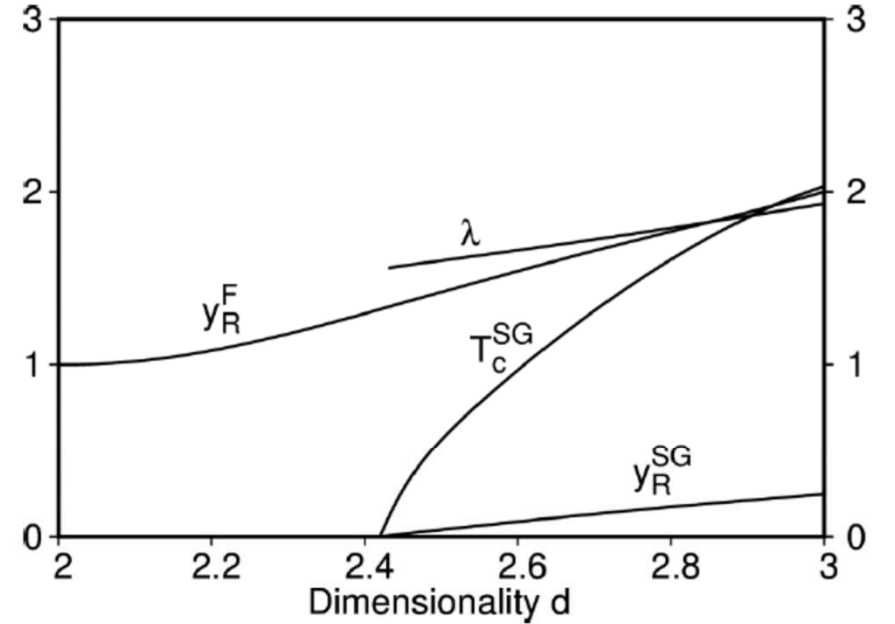


FIG. 6. Spin-glass critical temperature T_c^{SG} at $p = 0.5$, spin-glass chaos Lyapunov exponent λ , spin-glass-phase runaway exponent y_R^{SG} , and ferromagnetic-phase runaway exponent y_R^{F} , as a function of dimensionality d . Note that the ferromagnetic-phase runaway exponent y_R^{F} correctly tracks $d - 1$.

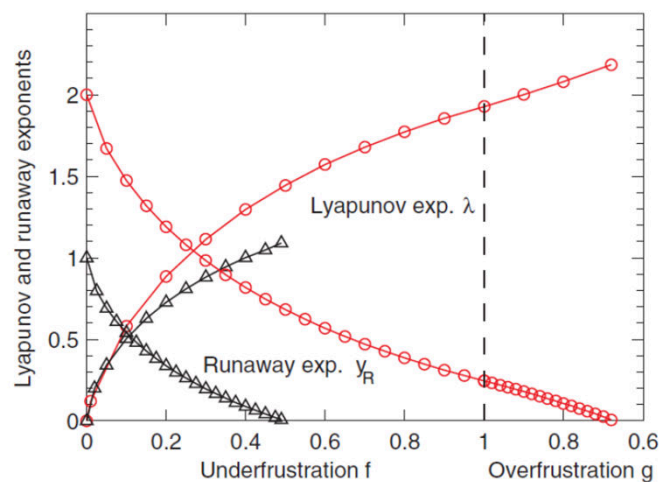
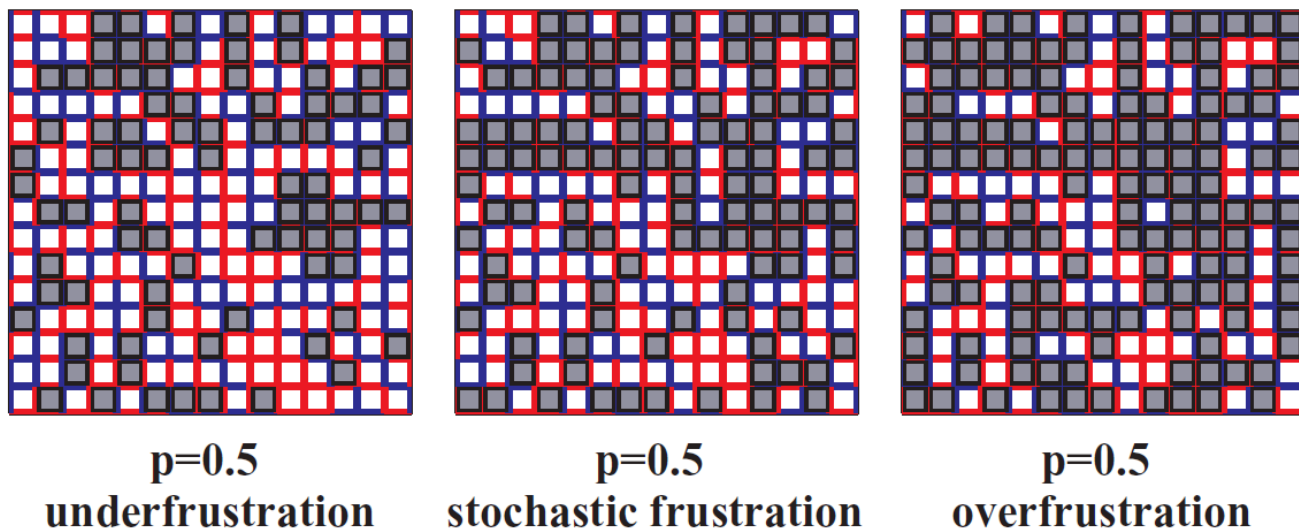


FIG. 10. (Color online) Lyapunov exponent λ and runaway exponent γ_R of the spin-glass phases of overfrustrated, underfrustrated, and stochastically frustrated Ising models in $d = 3$ (upper curves) and $d = 2$ (lower curves). The horizontal scale shows, to the left

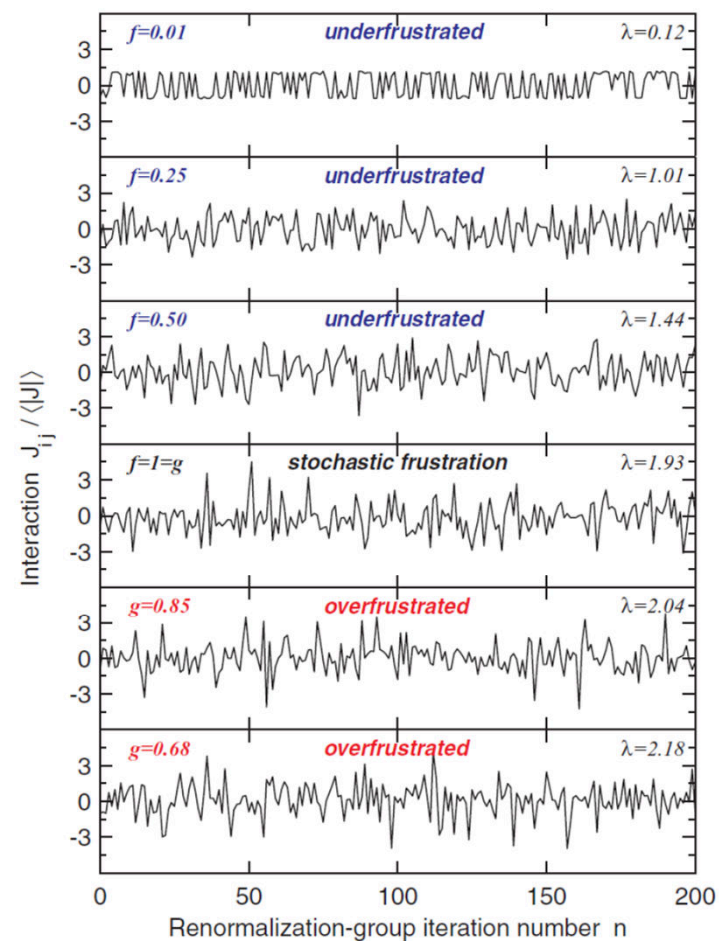


FIG. 6. (Color online) Interaction at a given position in the lattice at successive renormalization-group iterations, for $d = 3$ systems with different frustrations. In all cases, the antiferromagnetic bond concentration is $p = 0.5$ and the initial temperature is $1/J = 0.2$, inside the spin-glass phase. For each frustration amount, a chaotic trajectory of the interaction at a given position is seen. The calculated Lyapunov exponent for each case is given in the upper right corner of each panel.

Lower lower-critical spin-glass dimension from quenched mixed-spatial-dimensional spin glasses

Bora Atalay¹ and A. Nihat Berker^{2,3}

¹*Faculty of Engineering and Natural Sciences, Sabancı University, Tuzla, Istanbul 34956, Turkey*

²*Faculty of Engineering and Natural Sciences, Kadir Has University, Cibali, Istanbul 34083, Turkey*

³*Department of Physics, Massachusetts Institute of Technology, Cambridge, Massachusetts 02139, USA*



(Received 16 August 2018; published 15 October 2018)

By quenched-randomly mixing local units of different spatial dimensionalities, we have studied Ising spin-glass systems on hierarchical lattices continuously in dimensionalities $1 \leq d \leq 3$. The global phase diagram in temperature, antiferromagnetic bond concentration, and spatial dimensionality is calculated. We find that, as dimension is lowered, the spin-glass phase disappears to zero temperature at the lower-critical dimension $d_c = 2.431$. Our system being a physically realizable system, this sets an upper limit to the lower-critical dimension in general for the Ising spin-glass phase. As dimension is lowered towards d_c , the spin-glass critical temperature continuously goes to zero, but the spin-glass chaos fully subsists to the brink of the disappearance of the spin-glass phase. The Lyapunov exponent, measuring the strength of chaos, is thus largely unaffected by the approach to d_c and shows a discontinuity to zero at d_c .

DOI: [10.1103/PhysRevE.98.042125](https://doi.org/10.1103/PhysRevE.98.042125)

LÜTFEN DUYURU TAHTASINA ASINIZ

FAZ GEÇİŞLERİ ve RENORMALİZASYON GRUBU

(Massachusetts Institute of Technology Physics 8.334)

Lisans 3. ve 4. Sınıf ve Lisansüstü Öğrencilerine Yönelik Yoğun Programlı Ders

KADİR HAS ÜNİVERSİTESİ

Cibali Kampüsü (Haliç Metro durağı)

23 Eylül – 30 Aralık 2017

İlk ders: Cumartesi 23 Eylül 2017

Derse önceden kayıt gerekli değildir. İlk derse gelmeniz yeterlidir. Ders için hiç bir ücret yoktur.

Dersler: Cumartesileri 10:00 – 13:00 Prof. Dr. Nihat Berker, telefon: 0212-533-6386

nihatberker@khas.edu.tr, anberker@mit.edu

<http://webprs.khas.edu.tr/~nberker/>, <http://web.mit.edu/physics/berker>

Uygulamalar: Pazartesi 18:00 – 20:00 Bora Atalay ve Yunus Emre Bahar

Faz değişimlerinde oluşan ve evrensellik kuramıyla geniş alanda sistemlerde etkili, dikkate değer olgular incelenecektir. Bu olguları türetebilen, basit ve fiziksel yapıları teori öğretilecektir. Deney ve teori arasındaki dialog; ayrıca içgüdüsel, olgusal, yaklaşıklı, kesin ve sayısal yaklaşımların zengin buluşma noktaları örneklendirilecektir. Dersin sonunda, öğrenciler güncel araştırma sınırlarına ulaşmış olacaktır.

1. Giriş: faz diyagramları, termodinamik limit, kritik olgular, evrensellik.
2. Klasik teoriler, öztutarlılık: saf ortalama alan, yapılanmış ortalama alan, Landau kuramları; Ginzburg kriteri.
3. Ising modeli ve kesin çözümler: bir boyut; iki boyut; düalite; bütünsel faz diyagramları.
4. Kadanoff'un ölçeklenme teorisi.
5. Renormalizasyon grubu: Bir boyutta kesin çözümler.
6. Renormalizasyon grubu: İki boyutta yaklaşık çözümler. Termodinamik fonksiyonlar. Birinci tür faz geçişleri.
7. Migdal-Kadanoff dönüşümleri. Kesin çözümlü hiyerarşik örgüler. BEG modeli. Bütünsel çokkritik faz diyagramları.
8. Faz geçişi modelleri kullanarak: sinirsel ağlar, tavlama yakıştırmasıyla karmaşık sistem optimizasyonu, kodlama.
9. Donmuş düzensizlik ve etkileşme bunalımlığı altında düzen. Kaotik ölçeklenme ve spin camları. Küçük dünya ağları: geometrik ortam ve korelasyonlar arasında bağlantı.
10. Kuantum spin ve elektronik sistemlerinin renormalizasyon grubu. Elektron yerdeğişiminden gelen antiferromanyetizm. Safsızlıkların süperiletken ve antiferromanyetik fazlara değişik etkileri.

1. Giriş: faz diagramları, termodinamik limit, kritik olgular, evrensellik.
2. Klasik teoriler, öztutarlılık: saf ortalama alan, yapılanmış ortalama alan, Landau kuramları; Ginzburg kriteri.
3. Ising modeli ve kesin çözümler: bir boyut; iki boyut; düalite; bütünsel faz diyagramları.
4. Kadanoff'un ölçeklenme teorisi.
5. Renormalizasyon grubu: Bir boyutta kesin çözümler.
6. Renormalizasyon grubu: İki boyutta yaklaşık çözümler. Termodinamik fonksiyonlar. Birinci tür faz geçişleri.
7. Migdal-Kadanoff dönüşümleri. Kesin çözümlü hiyerarşik örgüler. BEG modeli. Bütünsel çokkritik faz diyagramları.
8. Faz geçişi modelleri kullanarak: sinirsel ağlar, tavlama yakıştırmasıyla karmaşık sistem optimizasyonu, kodlama.
9. Donmuş düzensizlik ve etkileşme bunalımlığı altında düzen. Kaotik ölçeklenme ve spin camları. Küçük dünya ağları: geometrik ortam ve korelasyonlar arasında bağlantı.
10. Kuantum spin ve elektronik sistemlerinin renormalizasyon grubu. Elektron yerdeğişiminden gelen antiferromanyetizm. Safsızlıkların süperiletken ve antiferromanyetik fazlara değişik etkileri.

Dersler Cumartesileri ve uygulamalar Pazartesileri yapılacaktır. Başarılı öğrencilere Üstün Başarı Sertifikası veya Başarı Sertifikası verilecektir.

Ayrıca, üstün başarılı öğrencilere, yayına yönelik özgün bir araştırma projesi geçmişte verilmiştir (**örnekler, bakınız <http://arxiv.org/abs/1602.00598>, <http://arxiv.org/abs/1502.06443>; bu makalelerdeki dersimizi almış lisans öğrencisi yazarlar, doktora çalışmalarını MIT ve Cornell Üniversitesinde devam ettirmektedir**) ve bu yıl da araştırma projesi verilebilir.

Derse Devam:

Derste her Cumartesi yazılı kısa sınav, her hafta bir ev ödevi, dönem ortasında ve sonunda yazılı ve sözlü sınavlar olacaktır.

Katılım için hiç bir ücret yoktur, ancak katılımcıların sınavları alıp ödevleri yapması kesinlikle beklenmektedir.

Nota katkı: kısa sınavlar 40%, ödevler 10%, yazılı sınavlar 35%, sözlü sınavlar 15%.

Devil's staircase continuum in the chiral clock spin glass with competing ferromagnetic-antiferromagnetic and left-right chiral interactions

Tolga Çağlar¹ and A. Nihat Berker^{1,2,3}

¹*Faculty of Engineering and Natural Sciences, Sabancı University, Tuzla, Istanbul 34956, Turkey*

²*Faculty of Engineering and Natural Sciences, Kadir Has University, Cibali, Istanbul 34083, Turkey*

³*Department of Physics, Massachusetts Institute of Technology, Cambridge, Massachusetts 02139, USA*

(Received 10 December 2016; revised manuscript received 10 February 2017; published 17 April 2017)

The chiral clock spin-glass model with $q = 5$ states, with both competing ferromagnetic-antiferromagnetic and left-right chiral frustrations, is studied in $d = 3$ spatial dimensions by renormalization-group theory. The global phase diagram is calculated in temperature, antiferromagnetic bond concentration p , random chirality strength, and right-chirality concentration c . The system has a ferromagnetic phase, a multitude of different chiral phases, a chiral spin-glass phase, and a critical (algebraically) ordered phase. The ferromagnetic and chiral phases accumulate at the disordered phase boundary and form a spectrum of devil's staircases, where different ordered phases characteristically intercede at all scales of phase-diagram space. Shallow and deep reentrances of the disordered phase, bordered by fragments of regular and temperature-inverted devil's staircases, are seen. The extremely rich phase diagrams are presented as continuously and qualitatively changing videos.

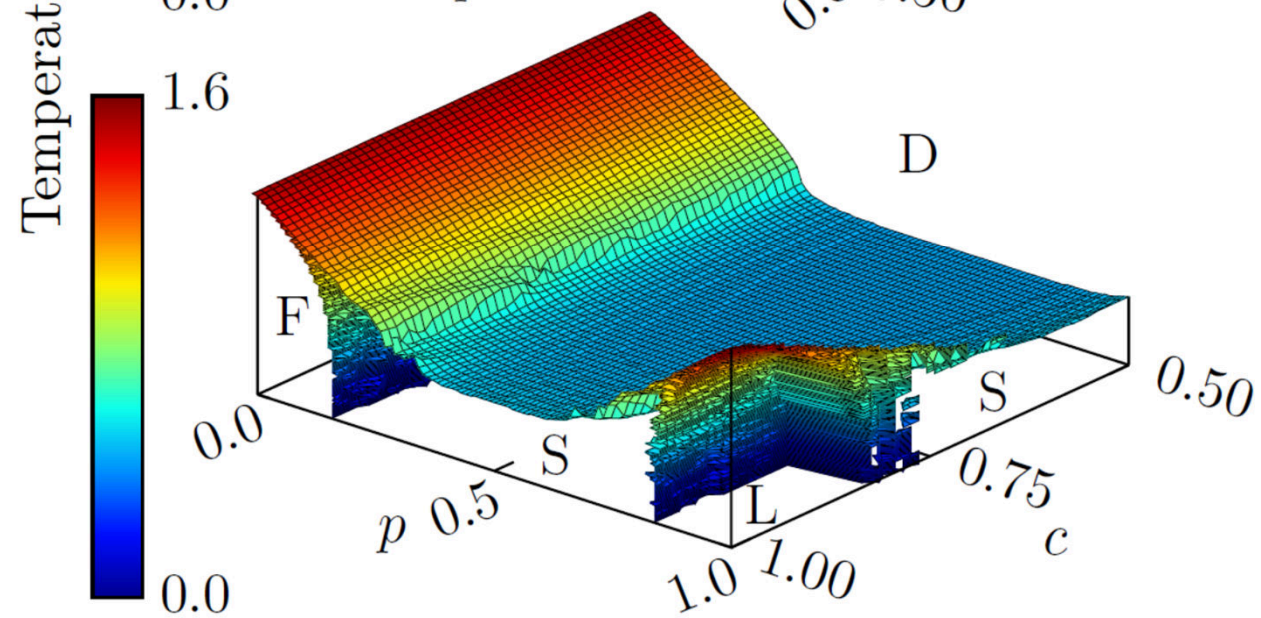
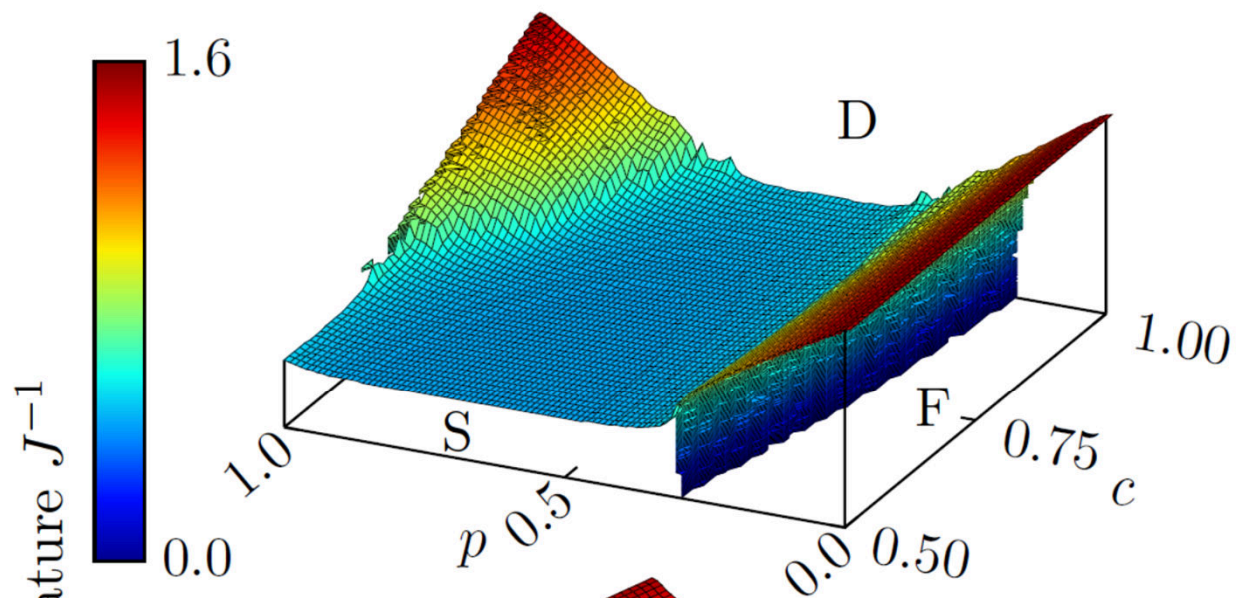
Chiral (Helical) Potts Spin-Glass System

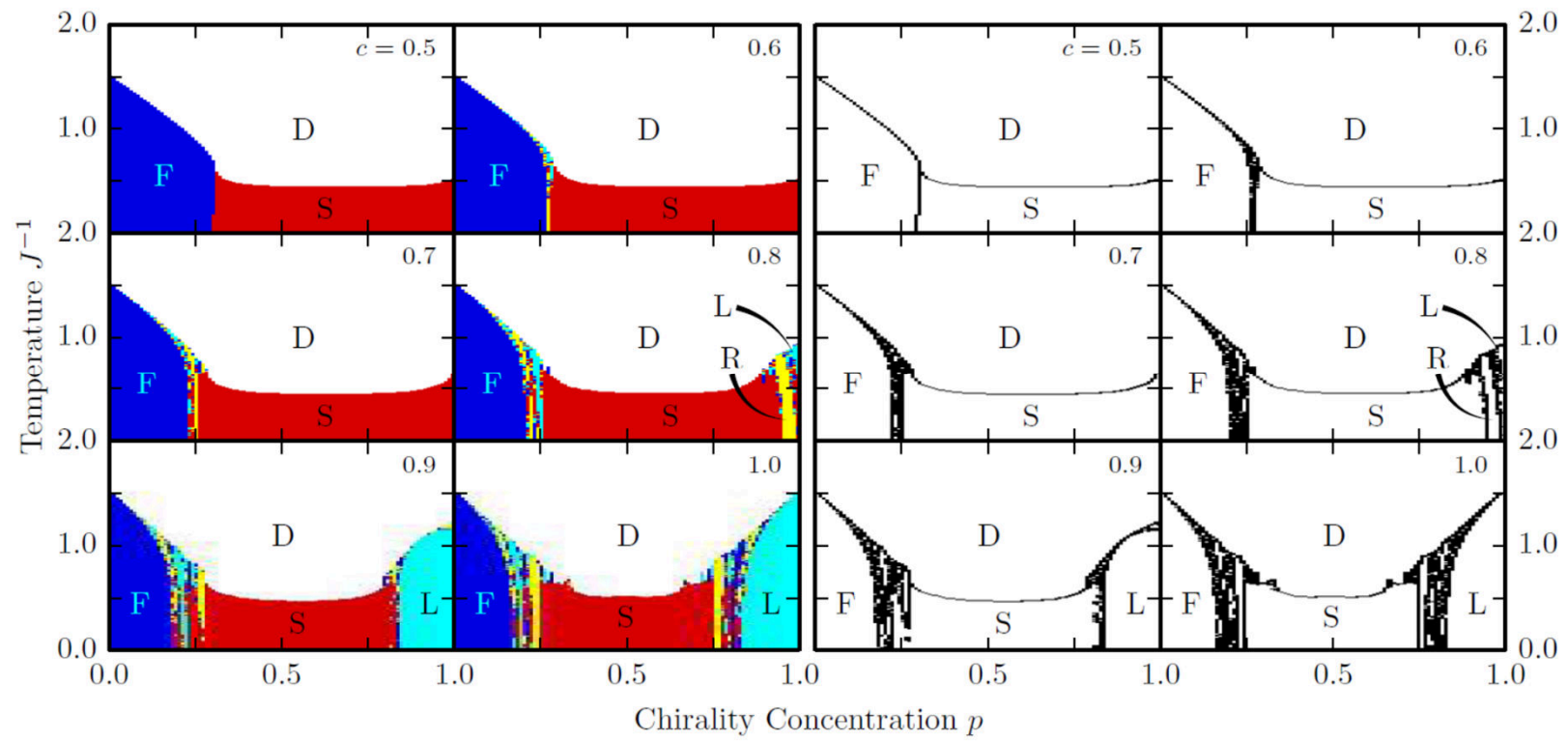
$$- \beta \mathcal{H} = \sum_{\langle ij \rangle} J [(1 - \eta_{ij}) \delta(s_i, s_j) + \eta_{ij} [\phi_{ij} \delta(s_i, s_j + 1) + (1 - \phi_{ij}) \delta(s_i, s_j - 1)]]$$

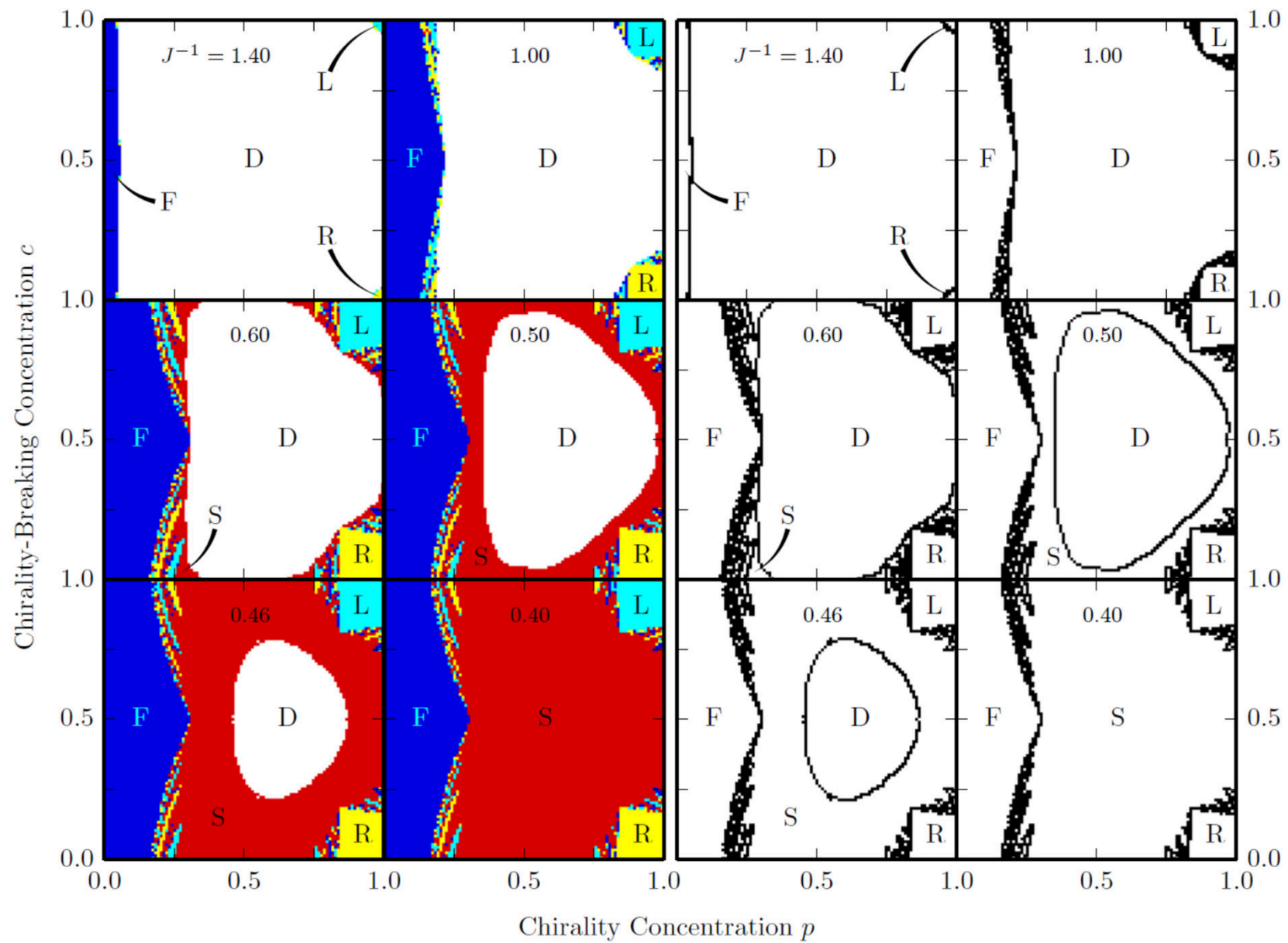
After renormalization-group transformation:

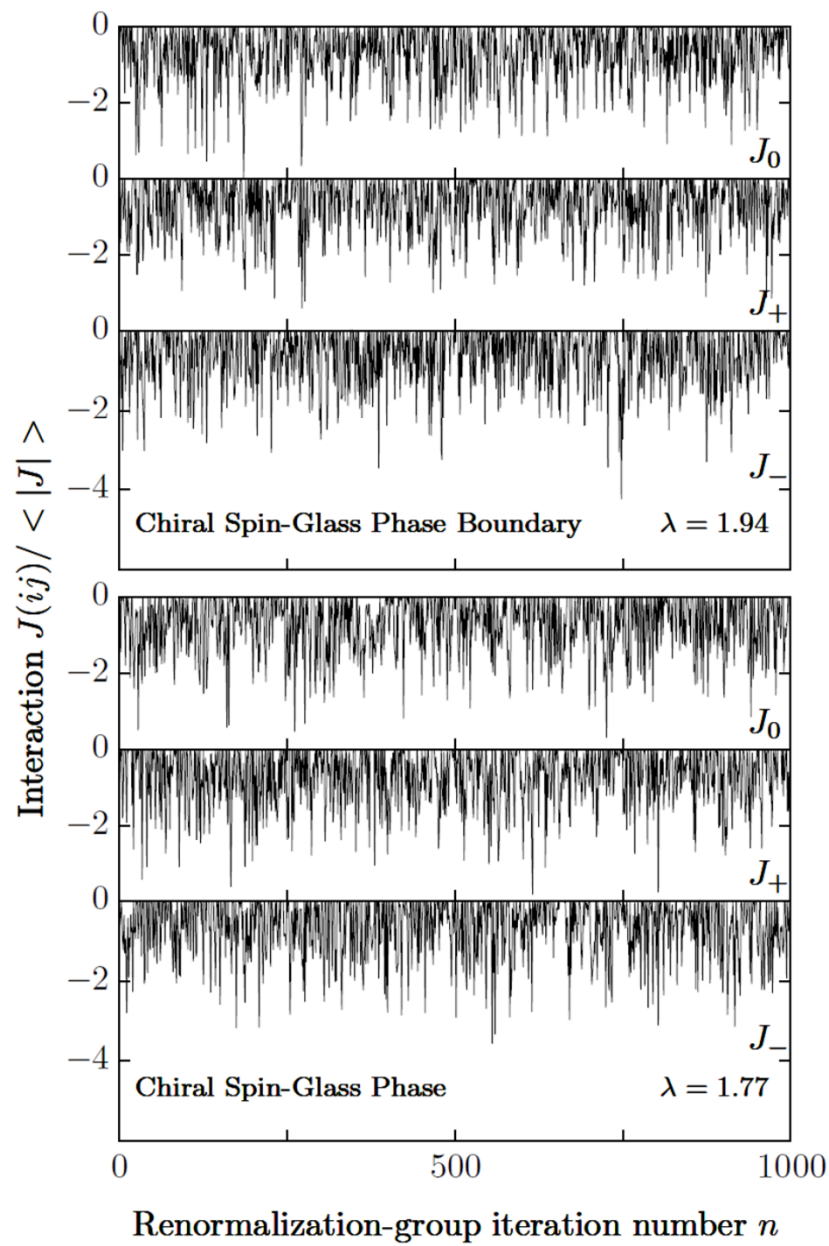
$$- \beta \mathcal{H} = \sum_{\langle ij \rangle} [J_0(ij) \delta(s_i, s_j) + J_+(ij) \delta(s_i, s_j + 1) + J_-(ij) \delta(s_i, s_j - 1)]$$

d = 3





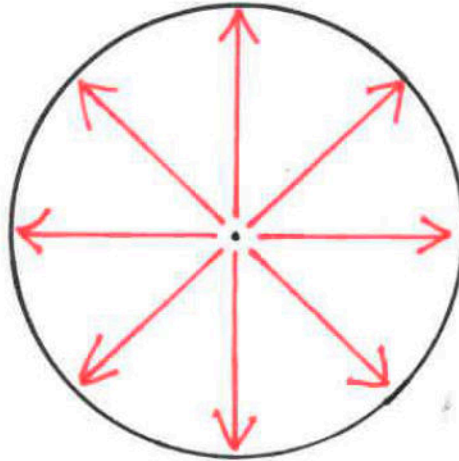




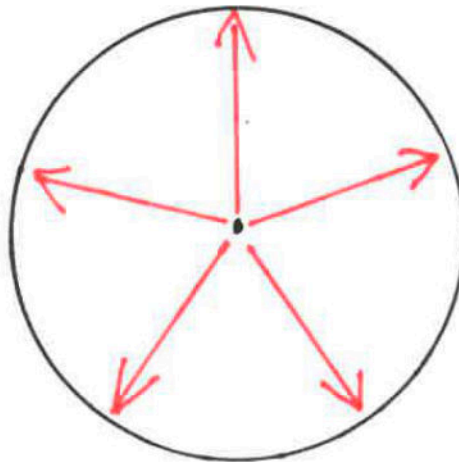
$$\lambda = \lim_{n \rightarrow \infty} \frac{1}{n} \sum_{k=0}^{n-1} \ln \left| \frac{dx_{k+1}}{dx_k} \right|$$

q-State Clock Spin Models

even q



odd q



Ground-state entropy

q-State Clock

$$-\beta\mathcal{H} = \sum_{\langle ij \rangle} J_{ij} \vec{s}_i \cdot \vec{s}_j = \sum_{\langle ij \rangle} J_{ij} \cos(\theta_i - \theta_j),$$

$$\theta_i = (2\pi/q) \sigma_i \quad \text{with } \sigma_i = 0, 1, 2, \dots, q$$

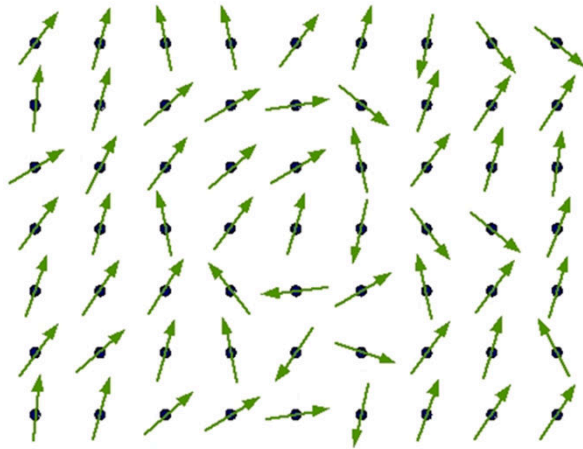
$$J_{ij} = +J \quad (\text{ferromagnetic}) \quad \text{with probability } 1-p$$

Spin-Glass Model

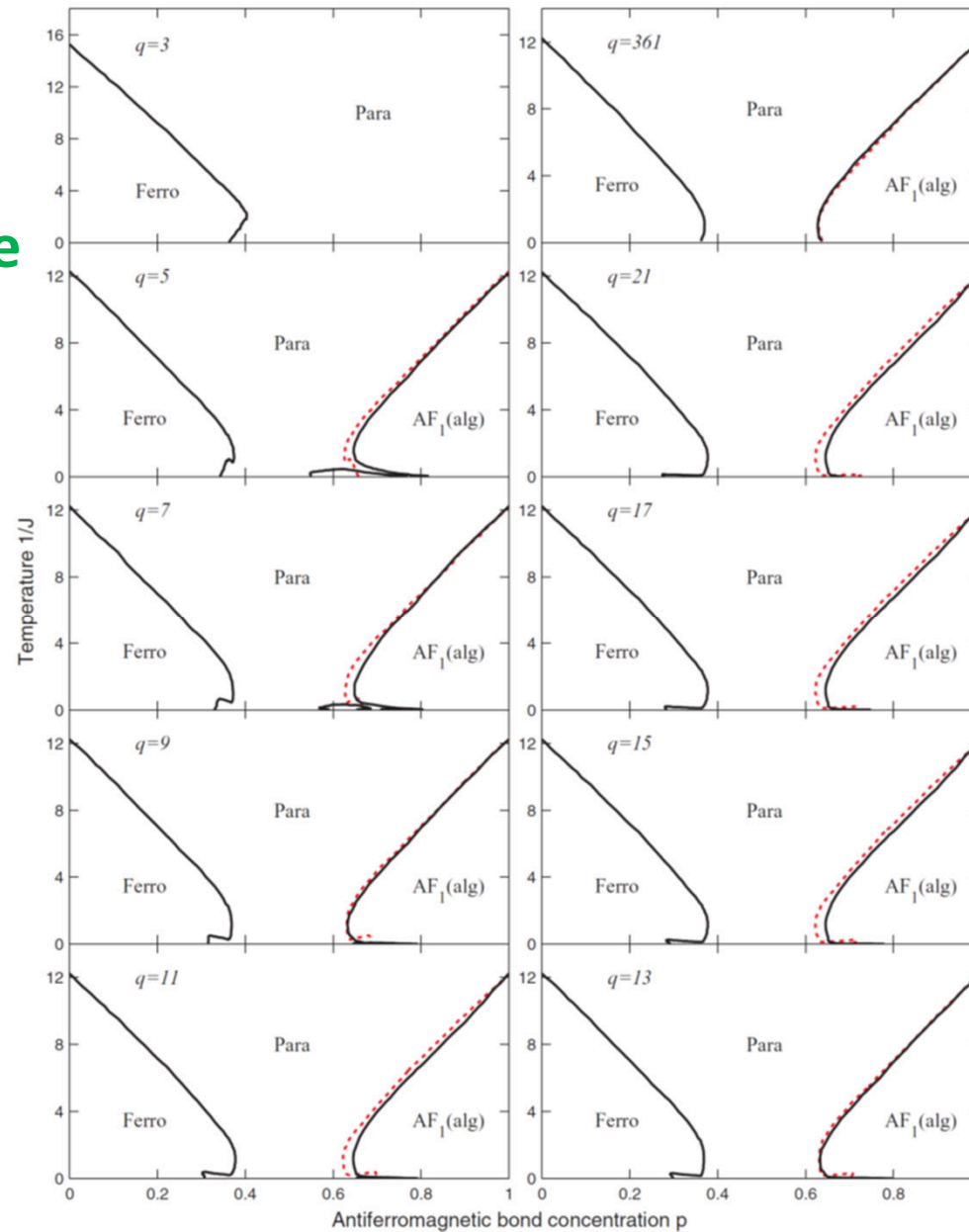
$$J_{ij} = -J \quad (\text{antiferromagnetic}) \quad \text{with probability } p$$

Under renormalization group, most general
potential

$$-\beta\mathcal{H} = \sum_{\langle ij \rangle} V_{ij}(\theta_i - \theta_j)$$



Odd q
Reentrance



Algebraic order
Most misaligned, next-most misaligned pairs dominate Entropy

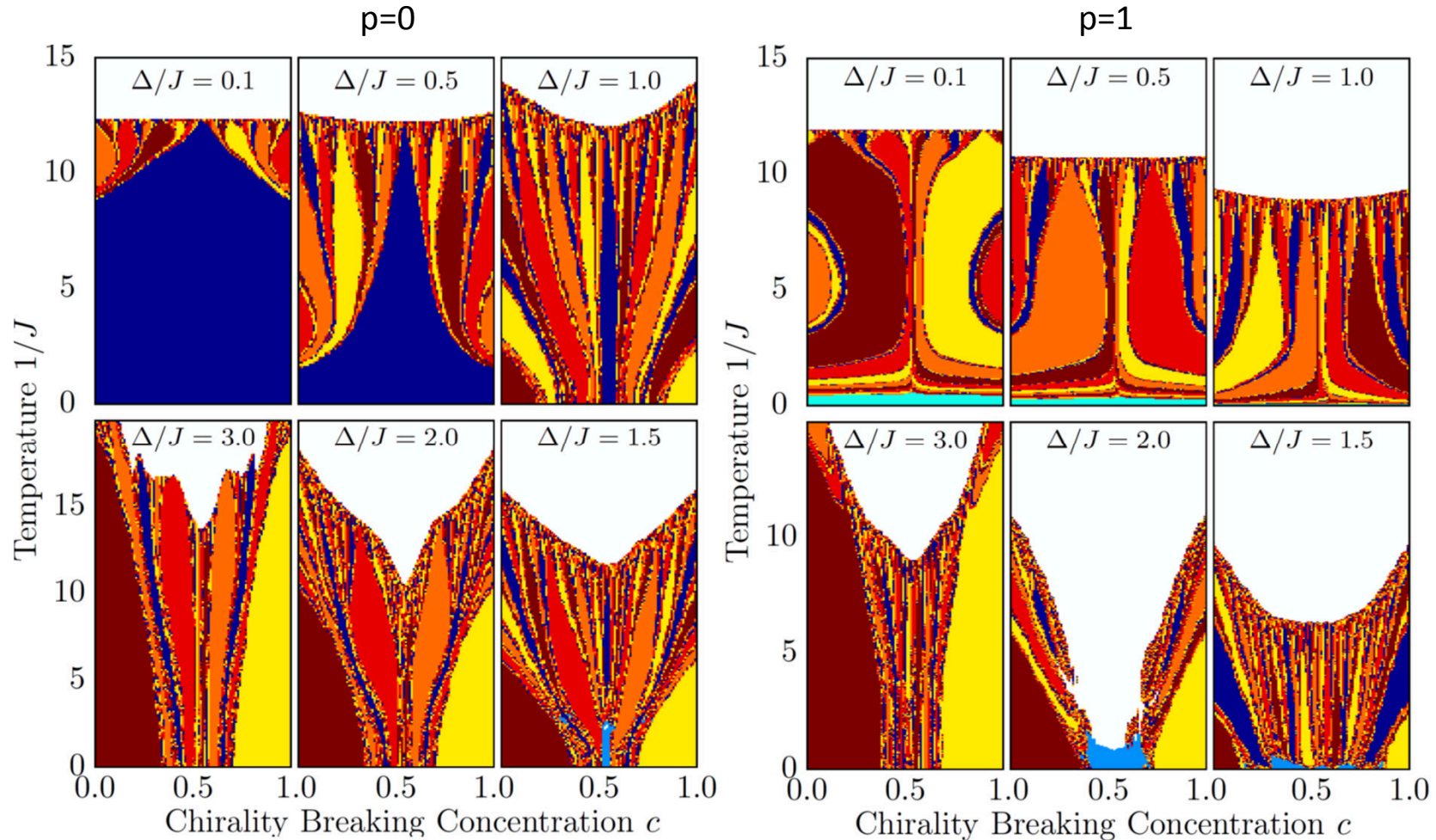
Asymmetric phase diagram

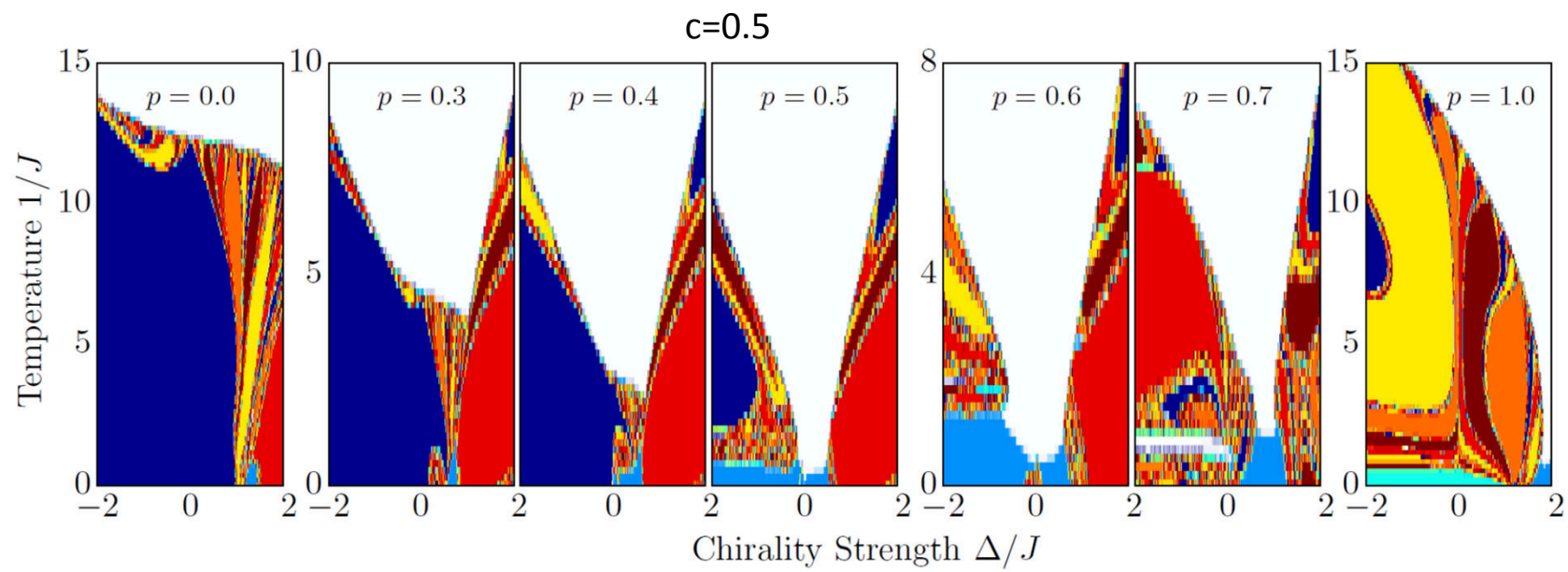
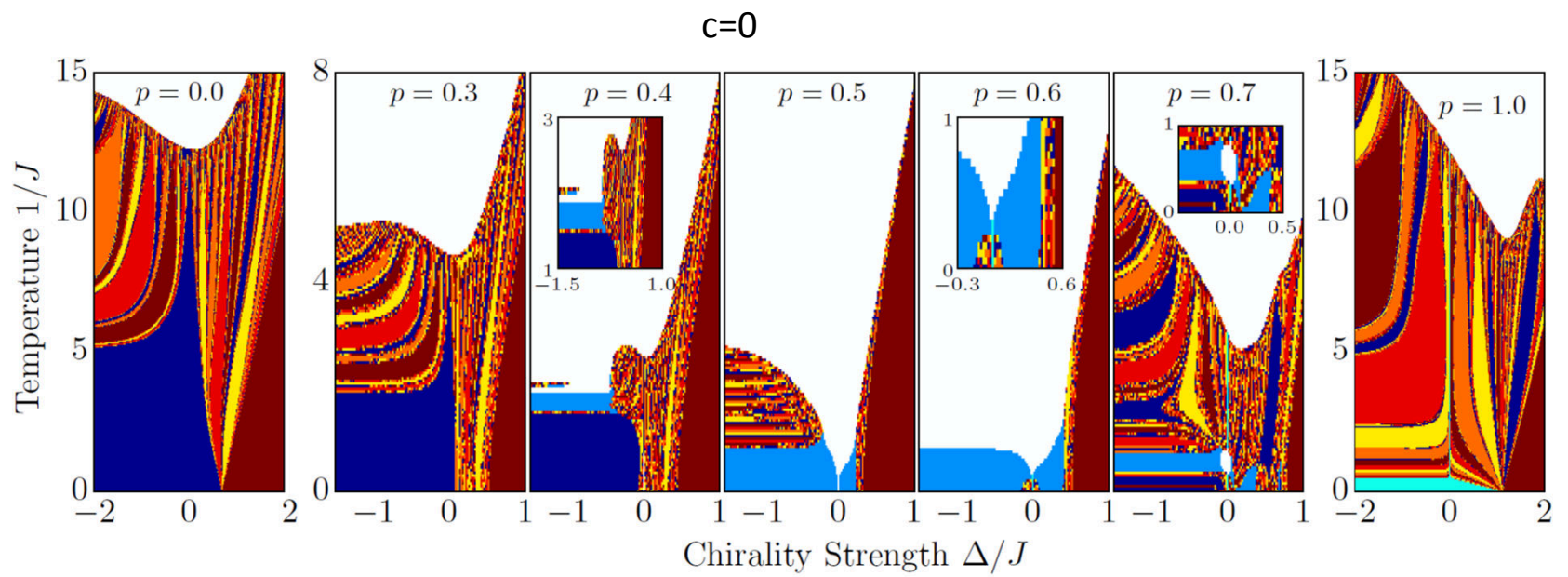
Ferro/Antiferro Right/Left Chiral Clock System

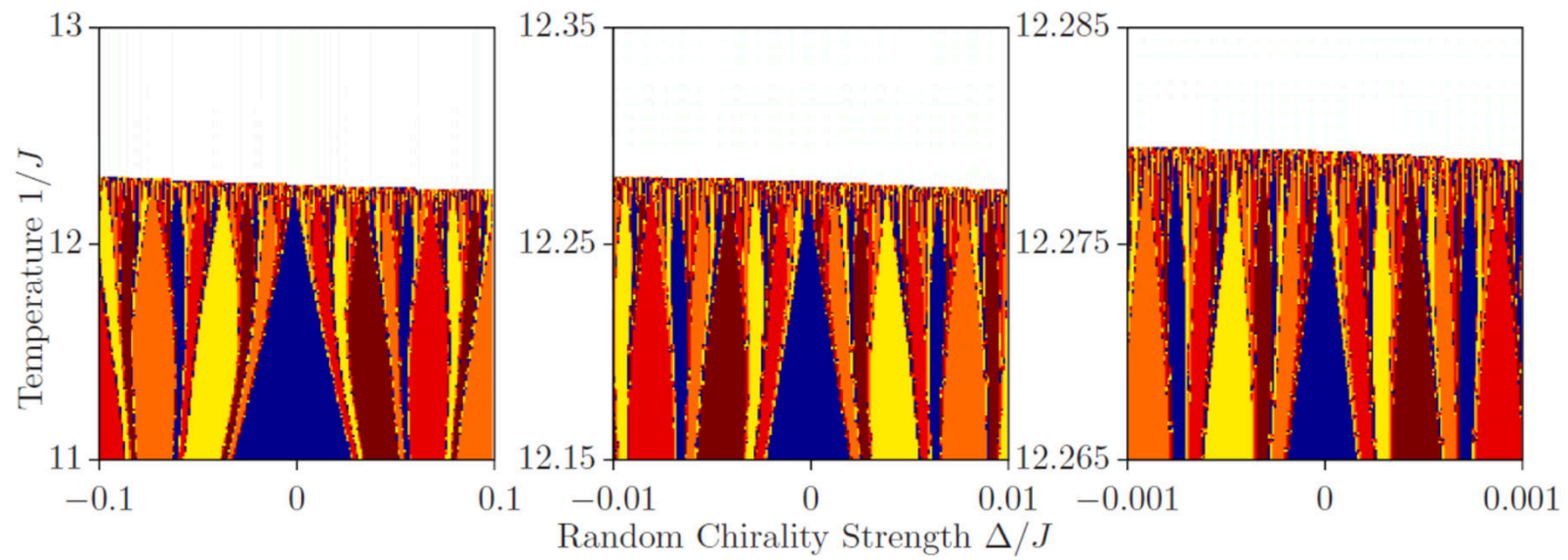
$$-\beta H = \sum_{\langle ij \rangle} \eta_{ij} J \cos \theta_{ij} + \Delta \delta(\theta_{ij} - \phi_{ij} \frac{2\pi}{q})$$

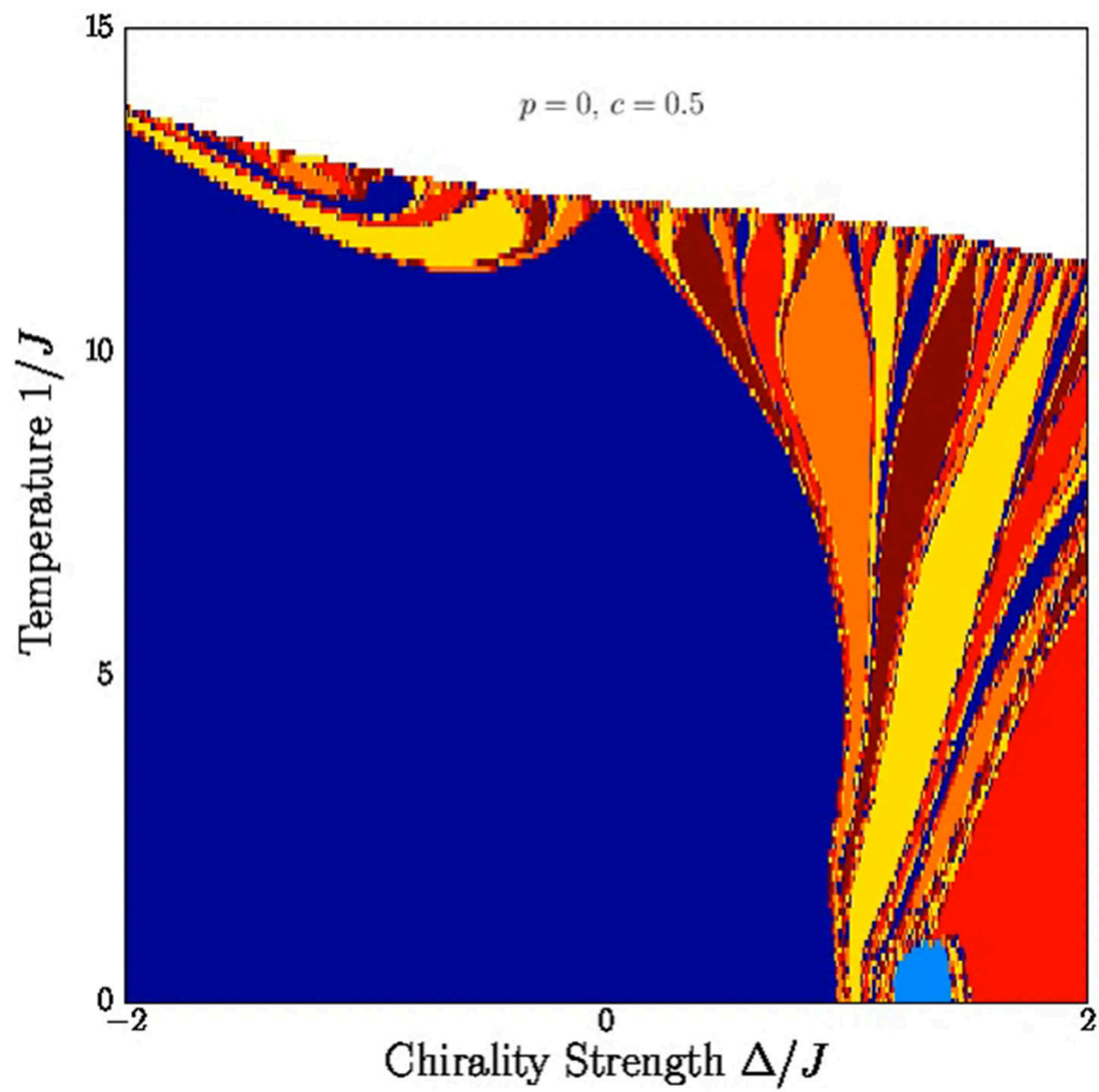
$\eta_{ij} = +/-1$ ferro/antiferro with p
 $\phi_{ij} = +/-1$ right/left chiral with c

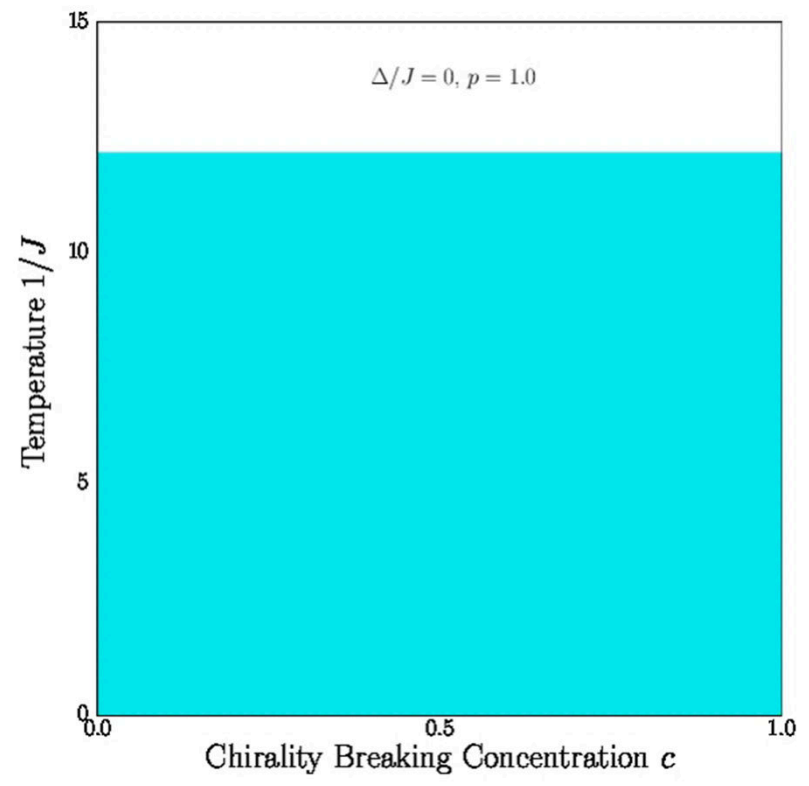
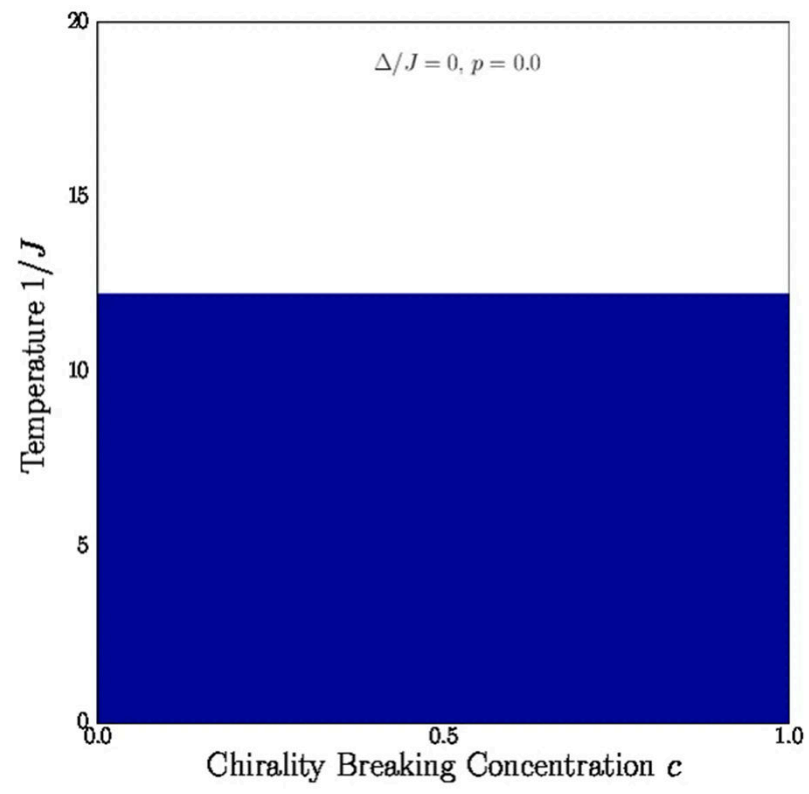
ODD $q=5$ states, $d=3$ dimensions







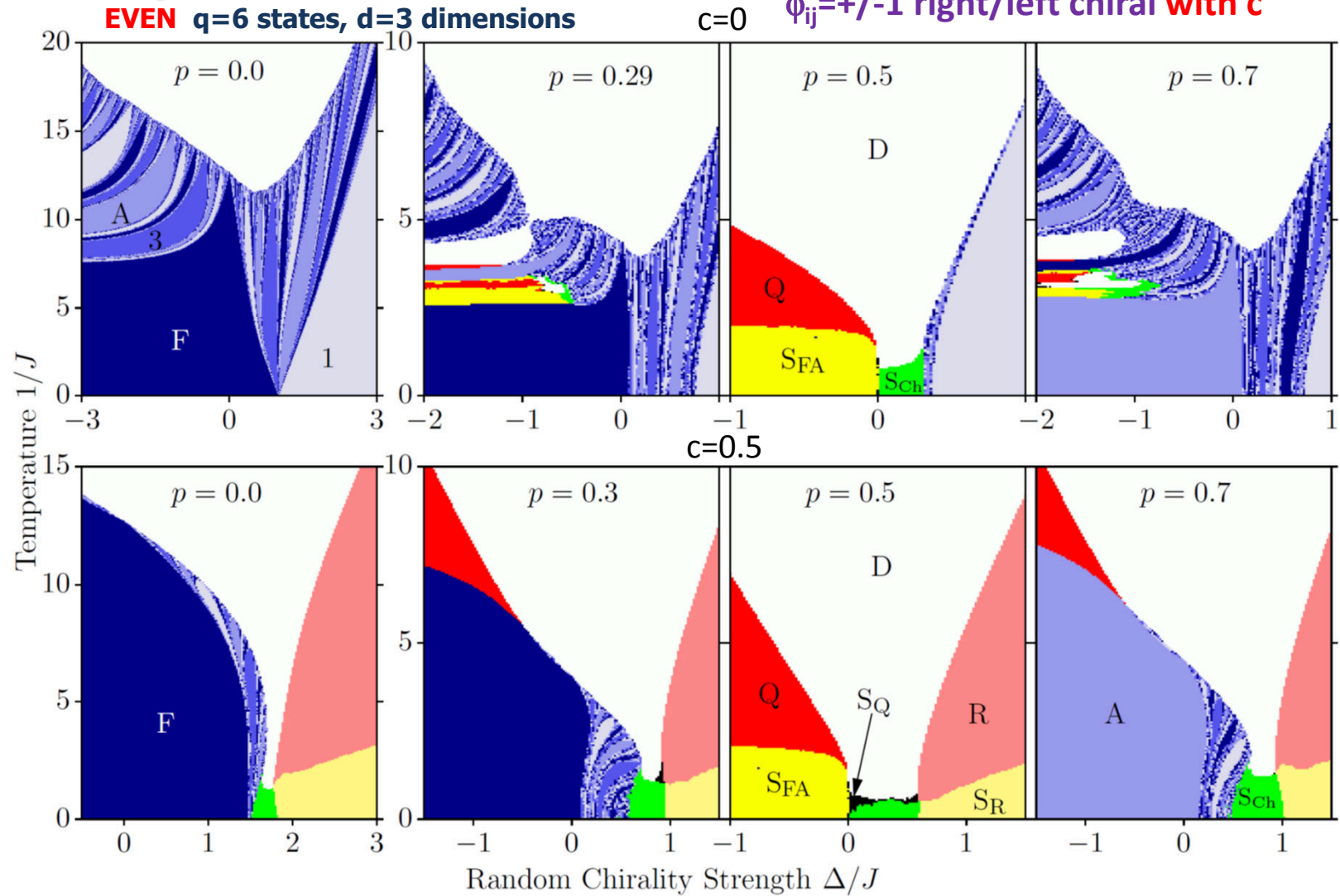


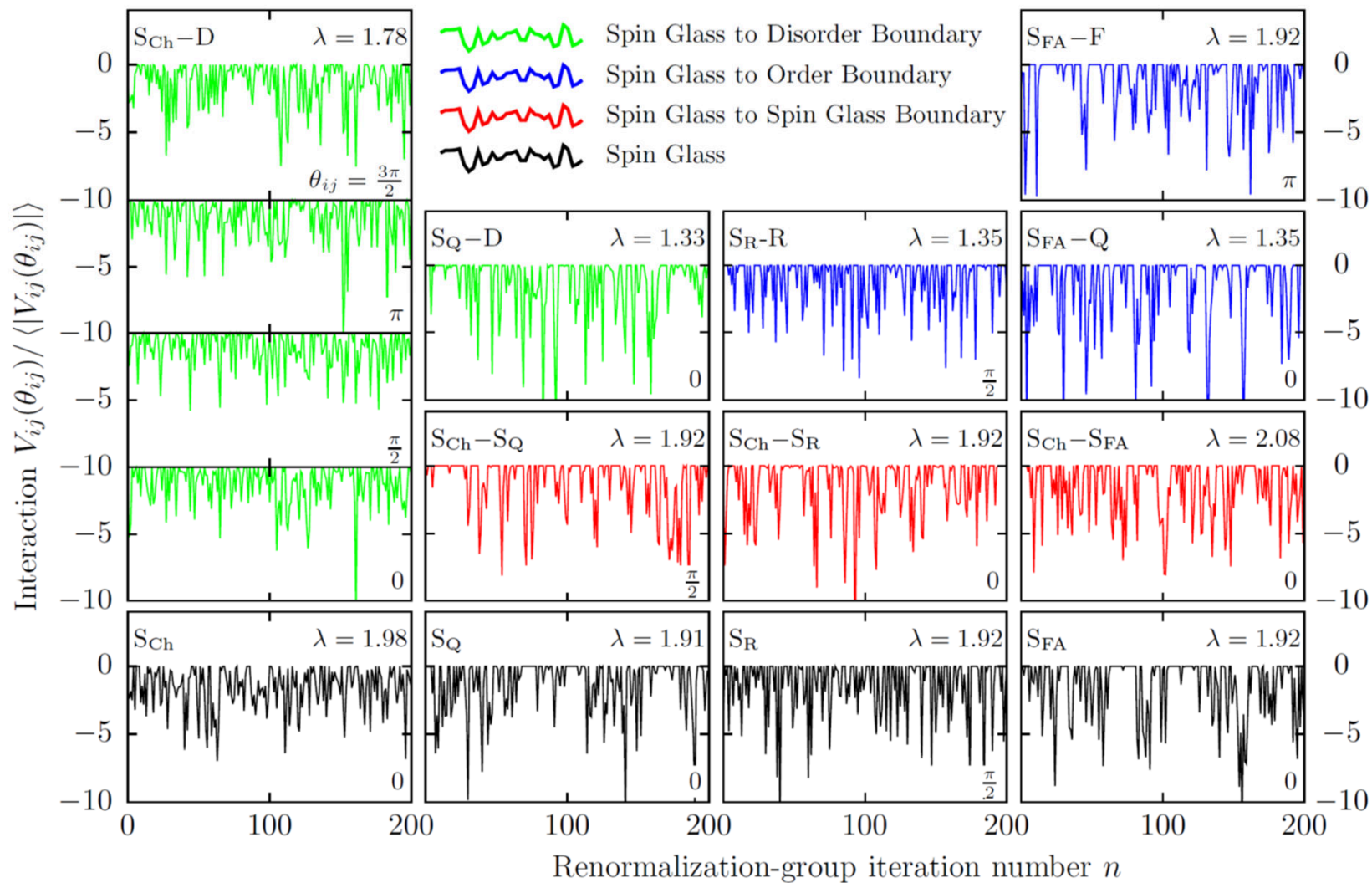


Ferro/Antiferro Right/Left Chiral Clock System

$$-\beta H = \sum_{\langle ij \rangle} \eta_{ij} J \cos \theta_{ij} + \Delta \delta(\theta_{ij} - \phi_{ij} \frac{2\pi}{q})$$

$\eta_{ij} = +/- 1$ ferro/antiferro with p
 $\phi_{ij} = +/- 1$ right/left chiral with c





Maximally random discrete-spin systems with symmetric and asymmetric interactions and maximally degenerate ordering

Bora Atalay¹ and A. Nihat Berker^{2,3}

¹*Faculty of Engineering and Natural Sciences, Sabancı University, Tuzla, Istanbul 34956, Turkey*

²*Faculty of Engineering and Natural Sciences, Kadir Has University, Cibali, Istanbul 34083, Turkey*

³*Department of Physics, Massachusetts Institute of Technology, Cambridge, Massachusetts 02139, USA*



(Received 20 January 2018; published 2 May 2018)

Discrete-spin systems with maximally random nearest-neighbor interactions that can be symmetric or asymmetric, ferromagnetic or antiferromagnetic, including off-diagonal disorder, are studied, for the number of states $q = 3, 4$ in d dimensions. We use renormalization-group theory that is exact for hierarchical lattices and approximate (Migdal-Kadanoff) for hypercubic lattices. For all $d > 1$ and all noninfinite temperatures, the system eventually renormalizes to a random single state, thus signaling $q \times q$ degenerate ordering. Note that this is the maximally degenerate ordering. For high-temperature initial conditions, the system crosses over to this highly degenerate ordering only after spending many renormalization-group iterations near the disordered (infinite-temperature) fixed point. Thus, a temperature range of short-range disorder in the presence of long-range order is identified, as previously seen in underfrustrated Ising spin-glass systems. The entropy is calculated for all temperatures, behaves similarly for ferromagnetic and antiferromagnetic interactions, and shows a derivative maximum at the short-range disordering temperature. With a sharp immediate contrast of infinitesimally higher dimension $1 + \epsilon$, the system is as expected disordered at all temperatures for $d = 1$.

$$-\beta\mathcal{H} = -\sum_{\langle ij \rangle} \beta\mathcal{H}_{ij},$$

$$\mathbf{T}_{ij} \equiv e^{-\beta\mathcal{H}_{ij}}$$

$$= \begin{pmatrix} 1 & e^J & 1 \\ 1 & 1 & e^J \\ e^J & 1 & 1 \end{pmatrix}, \begin{pmatrix} 1 & 1 & e^J \\ e^J & 1 & 1 \\ 1 & e^J & 1 \end{pmatrix}, \begin{pmatrix} e^J & 1 & 1 \\ 1 & 1 & e^J \\ 1 & e^J & 1 \end{pmatrix},$$

$$\begin{pmatrix} 1 & 1 & e^J \\ 1 & e^J & 1 \\ e^J & 1 & 1 \end{pmatrix}, \begin{pmatrix} 1 & e^J & 1 \\ e^J & 1 & 1 \\ 1 & 1 & e^J \end{pmatrix}, \text{ or } \begin{pmatrix} e^J & 1 & 1 \\ 1 & e^J & 1 \\ 1 & 1 & e^J \end{pmatrix},$$

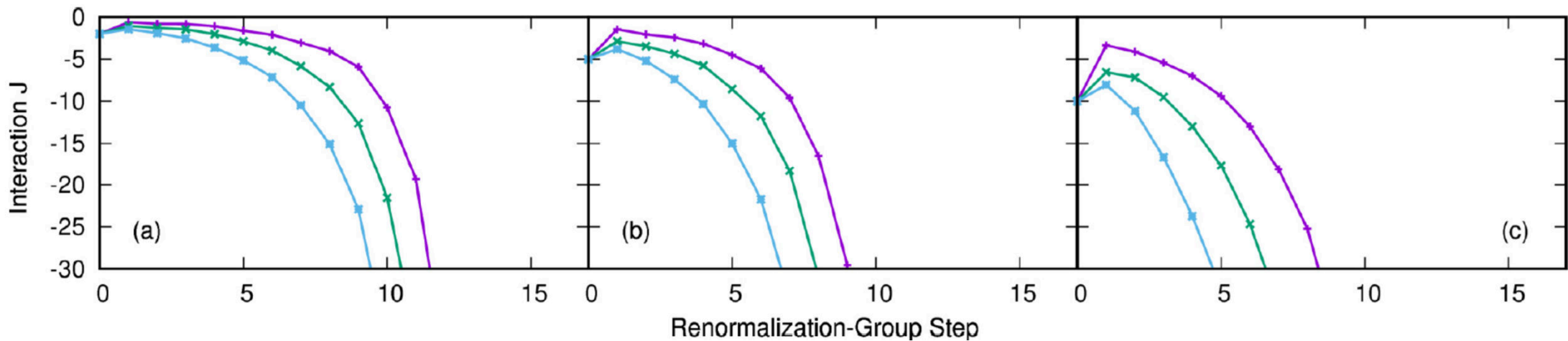


FIG. 1. Renormalization-group trajectories for the system with $q = 3$ states in $d = 3$ dimensions, starting at three different temperatures $T = J^{-1}$ from Eqs. (2) and (3), namely starting with (a) $J = 0.02$, (b) $J = 0.20$, (c) $J = 0.50$. Shown are the second (J_2) and third (J_3) largest values and the matrix average of the eight nonleading energies $\langle J_{2-9} \rangle$ of the transfer matrix [Eq. (4)], averaged over the quenched random distribution. The leading energy is $J_1 = 0$ by subtractive choice. The different starting values can be seen on the left axis of each panel

The renormalization-group solution gives the complete equilibrium thermodynamics for the systems studied. The dimensionless free energy per bond $f = F/kN$ is obtained by summing the additive constants generated at each renormalization-group step,

$$f = \frac{1}{N} \ln \sum_{\{s_i\}} e^{-\beta\mathcal{H}} = \sum_{n=1} \frac{G^{(n)}}{b^{dn}}, \quad (5)$$

where N is the number of bonds in the initial unrenormalized system, the first sum is over all states of the system, the second sum is over all renormalization-group steps n , $G^{(n)}$ is the additive constant generated at the n th renormalization-group transformation averaged over the quenched random distribution, and the sum quickly converges numerically.

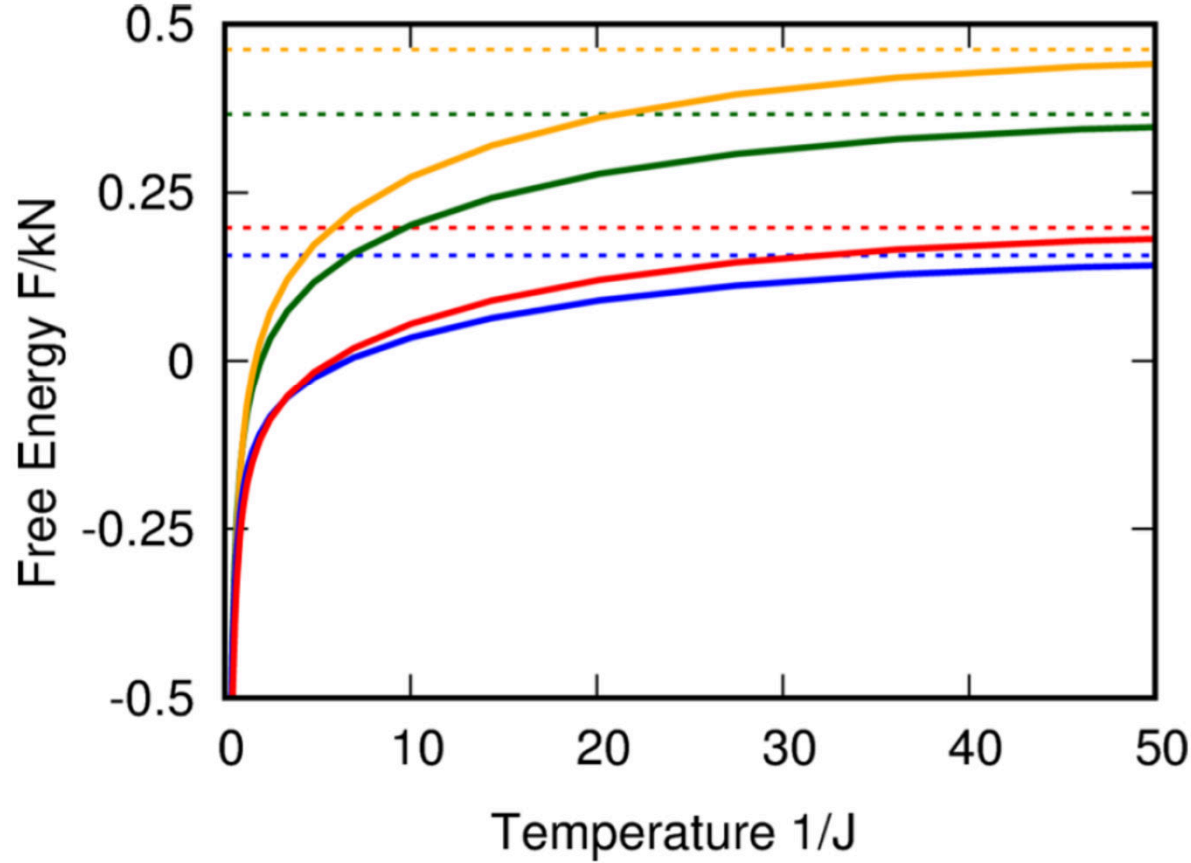


FIG. 2. Calculated free energy per bond as a function of temperature $T = J^{-1}$. The curves are, from top to bottom, for $(q = 4, d = 2)$, $(q = 3, d = 2)$, $(q = 4, d = 3)$, and $(q = 3, d = 3)$. The expected $T = \infty$ values of $f = F/kN = \ln q/(b^d - 1)$ are given by the dashed lines and match the calculations.

From the dimensionless free energy per bond f , the entropy per bond S/kN is calculated as

$$\frac{S}{kN} = f - J \frac{\partial f}{\partial J}, \quad (6)$$

and the specific heat C/kN is calculated as

$$\frac{C}{kN} = T \frac{\partial(S/kN)}{\partial T} = -J \frac{\partial(S/kN)}{\partial J}. \quad (7)$$

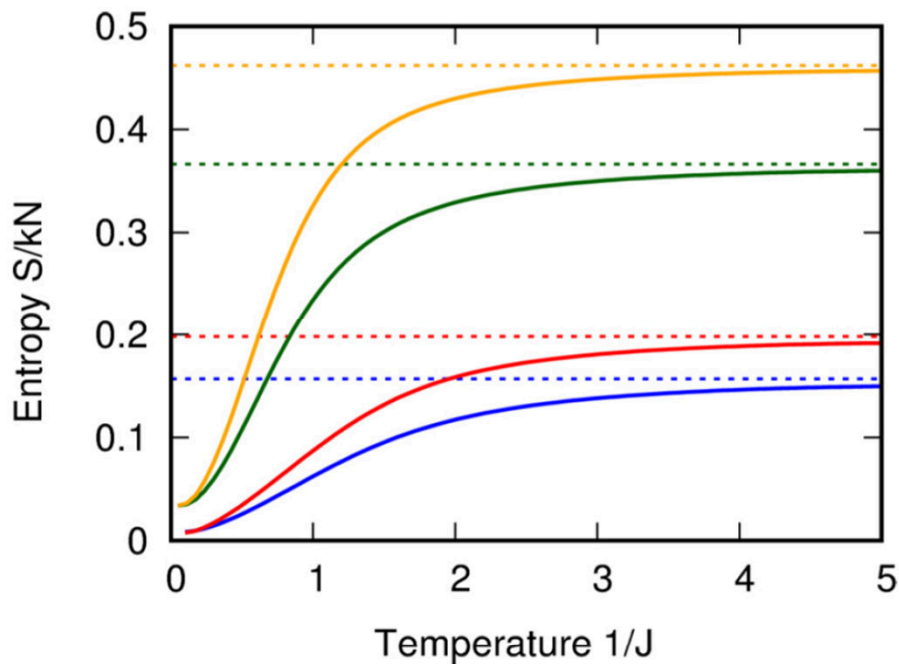


FIG. 3. Calculated entropy per bond as a function of temperature $T = J^{-1}$, for $q = 3, 4$ states in $d = 3, 4$ dimensions. The curves are, from top to bottom, for $(q = 4, d = 2)$, $(q = 3, d = 2)$, $(q = 4, d = 3)$, and $(q = 3, d = 3)$. The expected $T = \infty$ values of $S/kN = \ln q/(b^d - 1)$ are given by the dashed lines and match the calculations.

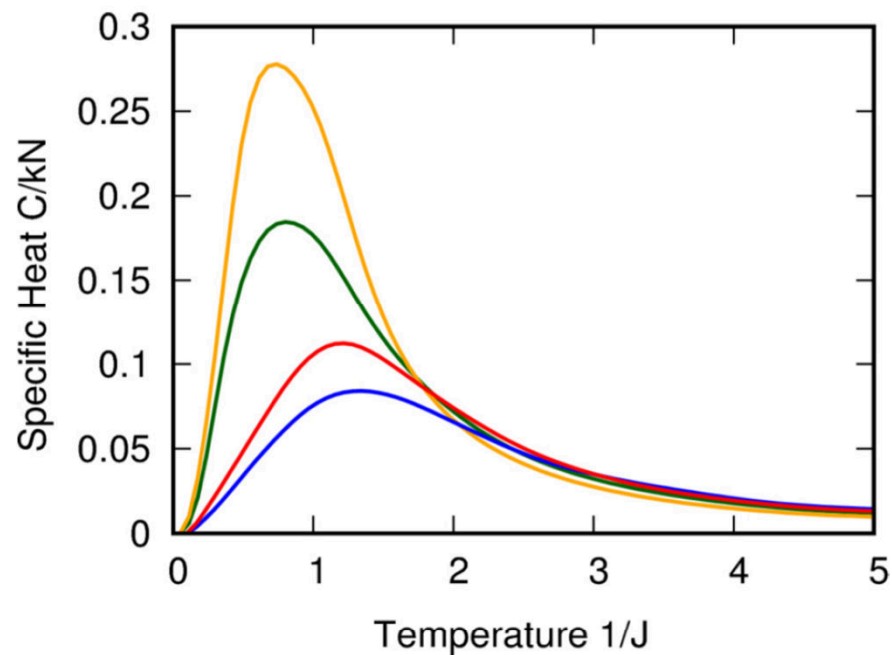


FIG. 4. Calculated specific heat as a function of temperature $T = J^{-1}$, for $q = 3, 4$ states in $d = 3, 4$ dimensions. The curves are, from top to bottom, for $(q = 4, d = 2)$, $(q = 3, d = 2)$, $(q = 4, d = 3)$, $(q = 3, d = 3)$. A specific heat maximum occurs at short-range disordering.

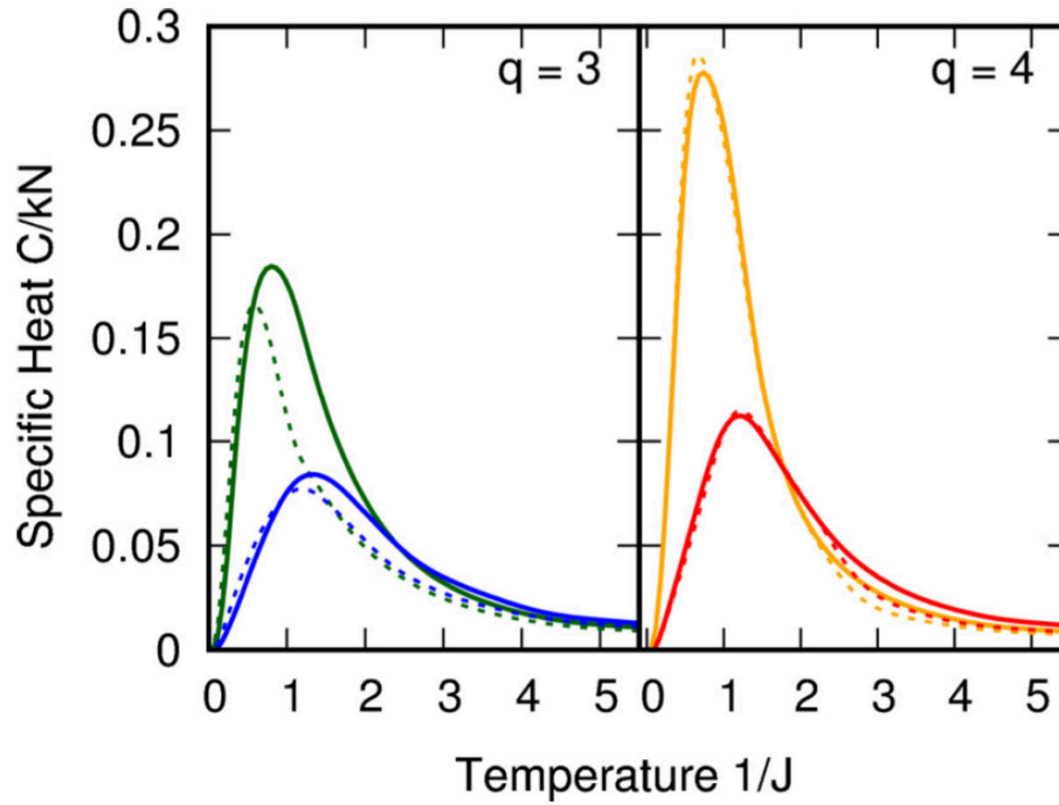


FIG. 5. Calculated specific heat as a function of temperature $T = |J|^{-1}$ for ferromagnetic ($J > 0$), full curves, and antiferromagnetic ($J < 0$), dashed curves, systems, for $q = 3, 4$ states in $d = 3, 4$ dimensions. The curves are, from top to bottom in each panel, for $d = 2$ and $d = 3$. The quantitatively same short-range disordering behavior is seen for both ferromagnetic and antiferromagnetic systems.

Overfrustrated and underfrustrated spin glasses in $d = 3$ and 2: Evolution of phase diagrams and chaos including spin-glass order in $d = 2$

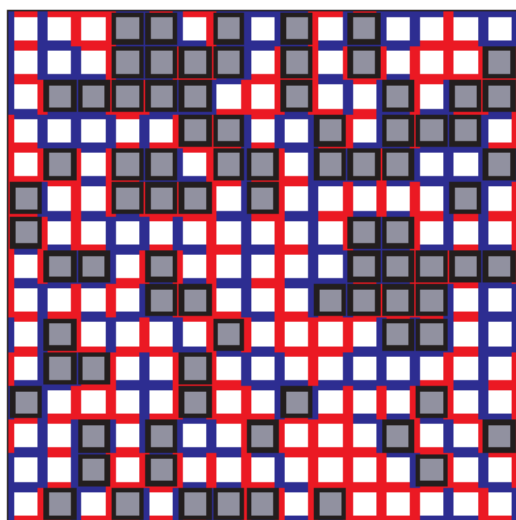
Efe Ilker¹ and A. Nihat Berker^{1,2}

¹*Faculty of Engineering and Natural Sciences, Sabancı University, Tuzla 34956, Istanbul, Turkey*

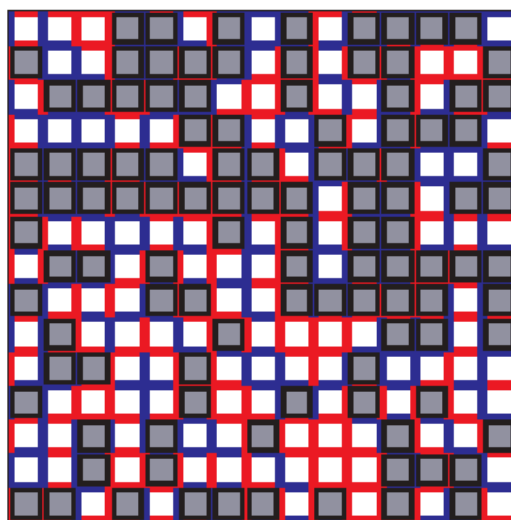
²*Department of Physics, Massachusetts Institute of Technology, Cambridge, Massachusetts 02139, USA*

(Received 27 November 2013; published 21 April 2014)

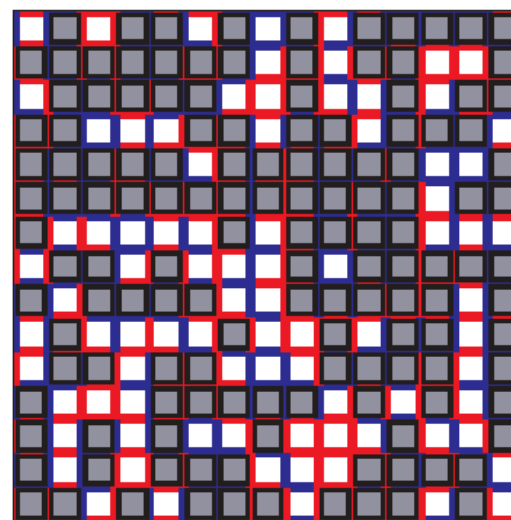
In spin-glass systems, frustration can be adjusted continuously and considerably, without changing the antiferromagnetic bond probability p , by using locally correlated quenched randomness, as we demonstrate here on hypercubic lattices and hierarchical lattices. Such overfrustrated and underfrustrated Ising systems on hierarchical lattices in $d = 3$ and 2 are studied. With the removal of just 51% of frustration, a spin-glass phase occurs in $d = 2$. With the addition of just 33% frustration, the spin-glass phase disappears in $d = 3$. Sequences of 18 different phase diagrams for different levels of frustration are calculated in both dimensions. In general, frustration lowers the spin-glass ordering temperature. At low temperatures, increased frustration favors the spin-glass phase (before it disappears) over the ferromagnetic phase and symmetrically the antiferromagnetic phase. When any amount, including infinitesimal, frustration is introduced, the chaotic rescaling of local interactions occurs in the spin-glass phase. Chaos increases with increasing frustration, as can be seen from the increased positive value of the calculated Lyapunov exponent λ , starting from $\lambda = 0$ when frustration is absent. The calculated runaway exponent y_R of the renormalization-group flows decreases with increasing frustration to $y_R = 0$ when the spin-glass phase disappears. From our calculations of entropy and specific-heat curves in $d = 3$, it is shown that frustration lowers in temperature the onset of both long- and short-range order in spin-glass phases, but is more effective on the former. From calculations of the entropy as a function of antiferromagnetic bond concentration p , it is shown that the ground-state and low-temperature entropy already mostly sets in within the ferromagnetic and antiferromagnetic phases, before the spin-glass phase is reached.



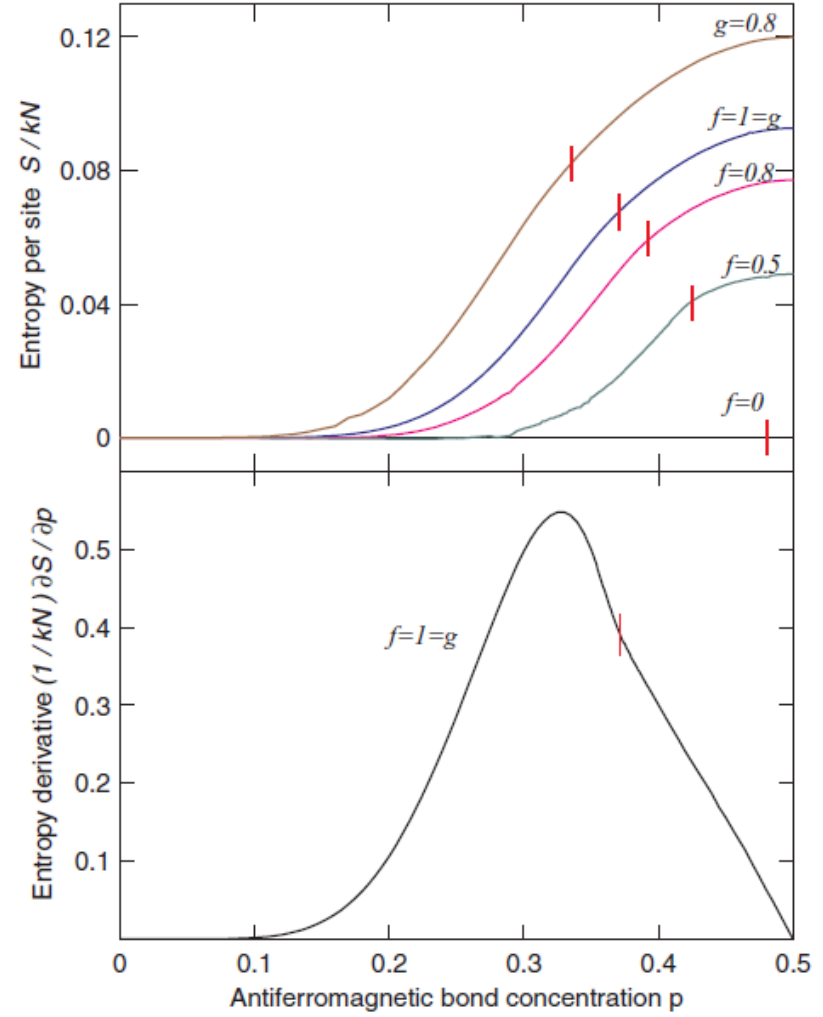
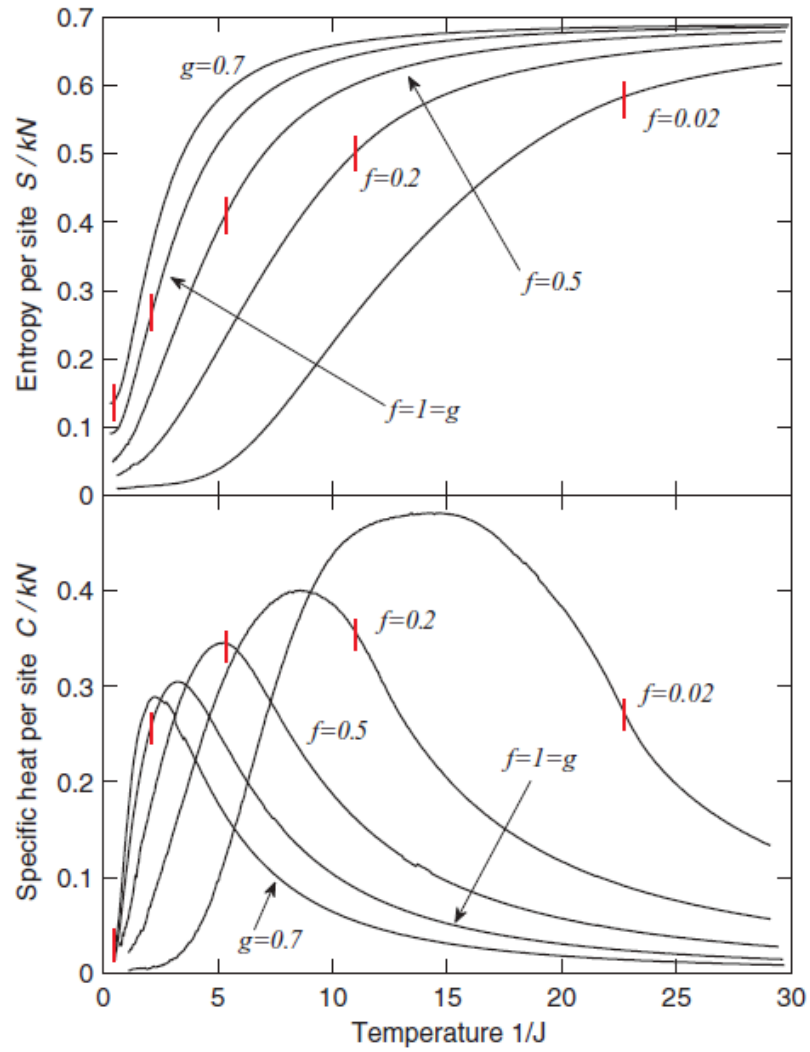
$p=0.5$
underfrustration



$p=0.5$
stochastic frustration



$p=0.5$
overfrustration



Short-range order and long-range order

Superfluidity and phase separation in helium films

A. N. Berker and David R. Nelson

Department of Physics, Harvard University,

Cambridge, Massachusetts 02138

(Received 28 September 1978)

A vectorial generalization of the Blume-Emery-Griffiths model is proposed to describe superfluidity in films of ^3He - ^4He mixtures, and is solved by an approximate renormalization scheme due to Migdal. In contrast to bulk mixtures, the line of superfluid transitions is connected to the phase-separation curve by a critical end point. The universal jump of the superfluid density, present in the pure ^4He system, is preserved with increasing ^3He concentrations x until the critical end point occurs at $x \leq 0.12$. At smaller x , phase separation causes a kink in the superfluid density versus temperature curve. No tricritical point occurs for any value of the model parameters, although an effectively tricritical phase diagram is obtained in a certain limit. Lines of constant superfluid density bunch up near the effective tricritical point, as predicted by tricritical scaling theory. This treatment also describes superfluidity in pure ^4He films in the presence of two-dimensional liquid-gas phase separation. In addition we calculate the specific heat of the pure ^4He system, using the recursion relations of Kosterlitz. This specific heat has a broad maximum above the superfluid transition temperature, corresponding to a gradual dissociation of vortex pairs with increasing temperature.

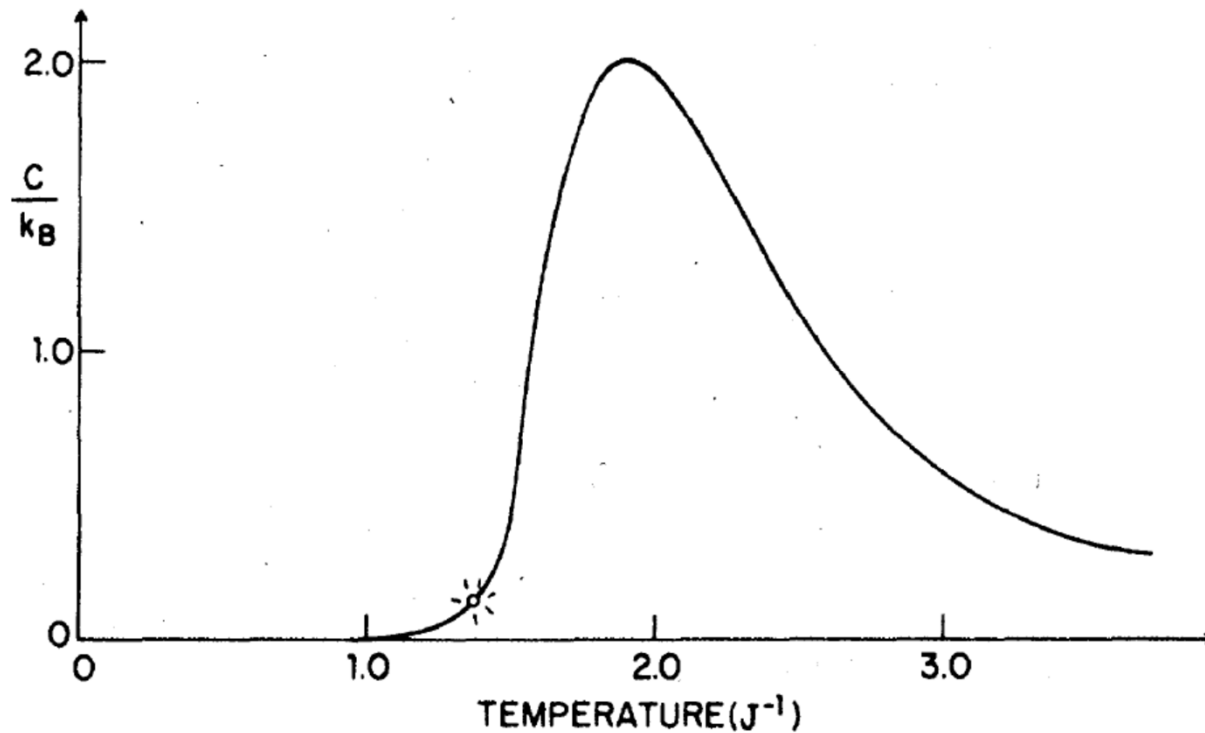


FIG. 5. Vortex contribution to the specific heat of a pure XY model in two demensions. The coupling J is the ratio of the nearest-neighbor interaction energy to $-k_B T$. The circle marks the phase transition temperature, where vortex unbinding first occurs. The specific heat has an unobservable essential singularity at this point.

“A **Lower Lower-Critical Spin-Glass Dimension** from Quenched Mixed-Spatial-Dimensional Spin Glasses”

B. Atalay and A.N. Berker, Phys. Rev. E 98, 042125, 1-5 (2018).

“**Maximally Random Discrete-Spin Systems** with Symmetric and Asymmetric Interactions and **Maximally Degenerate Ordering**”

B. Atalay and A.N. Berker, Phys. Rev. E 97, 052102, 1-5 (2018).

“Phase Transitions between **Different Spin-Glass Phases** and **between Different Chaoses** in Quenched Random Chiral Systems”

T. Çağlar and A.N. Berker, Phys. Rev. E 96, 032103, 1-6 (2017).

“The **Devils’s Staircase Phase Diagrams** in a Chiral Clock Spin Glass”

T. Çağlar and A.N. Berker, Phys. Rev. E 95, 042125, 1-8 (2017).

“The **Chiral Potts Spin Glass** in $d=2$ and 3 Dimensions”

T. Çağlar and A.N. Berker, Phys. Rev. E 94, 032121, 1-8 (2016).

“**Lower-Critical Spin-Glass Dimension** from 23 Sequenced Hierarchical Models”

M. Demirtaş, A. Tuncer, and A.N. Berker, Phys. Rev. E 92, 022136, 1-5 (2015).

“Odd q -State Clock Spin-Glass Models in Three Dimensions, Asymmetric Phase Diagrams, and **Multiple Algebraically Ordered Phases**”

E. Ilker and A.N. Berker, Phys. Rev. E 90, 062112, 1-7 (2014).

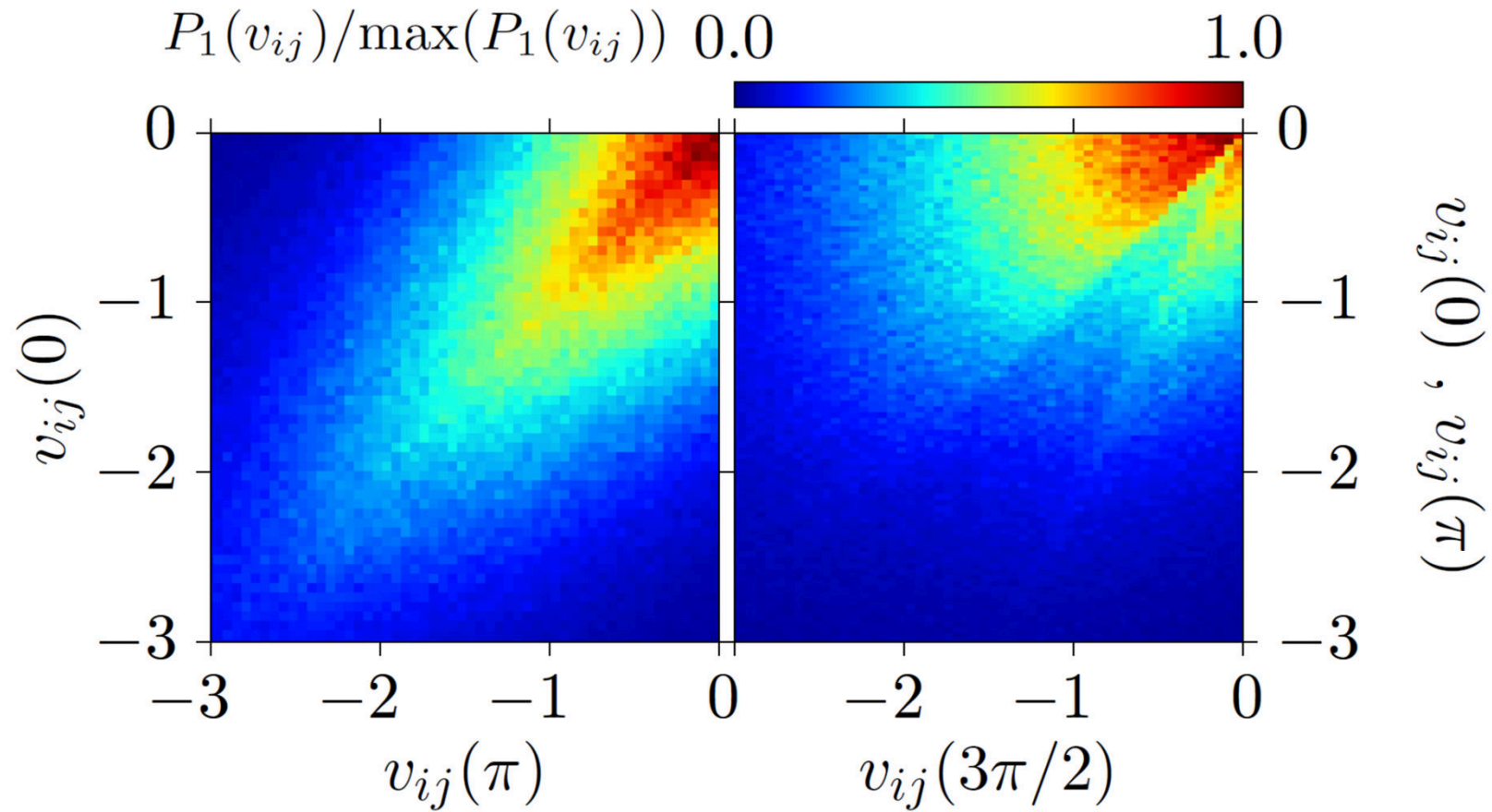
“**Overfrustrated and Underfrustrated Spin Glasses** in $d=3$ and 2: Evolution of Phase Diagrams and Chaos Including **Spin-Glass Order in $d=2$** ”

E. Ilker and A.N. Berker, Phys. Rev. E 89, 042139, 1-11 (2014).

“High q -State Clock Spin Glasses in Three Dimensions and the Lyapunov Exponents of **Chaotic Phases and Chaotic Phase Boundaries**”

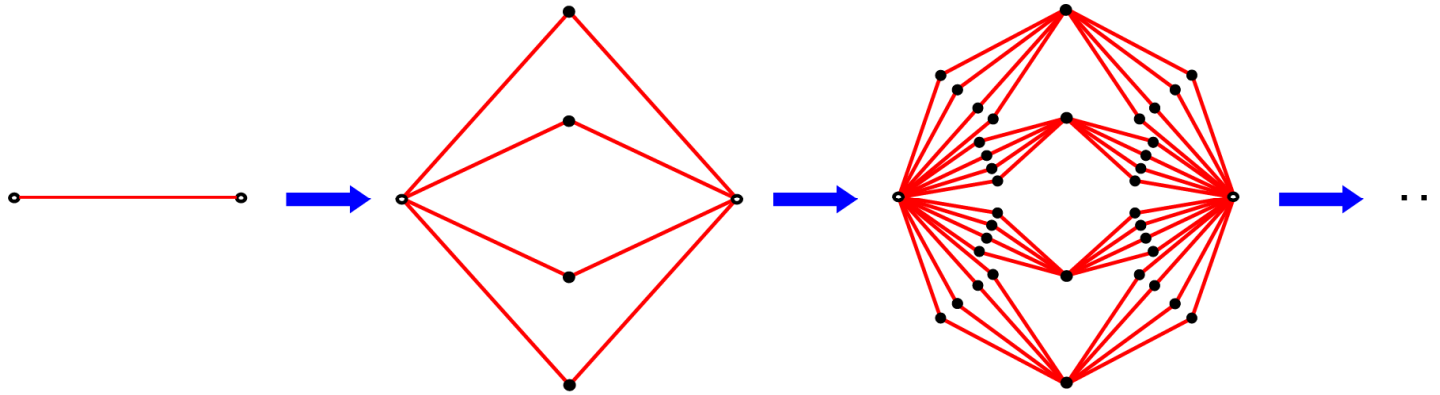
E. Ilker and A.N. Berker, Phys. Rev. E 87, 032124, 1-7 (2013).

Chiral Clock Spin-Glass Asymptotic Fixed Distribution

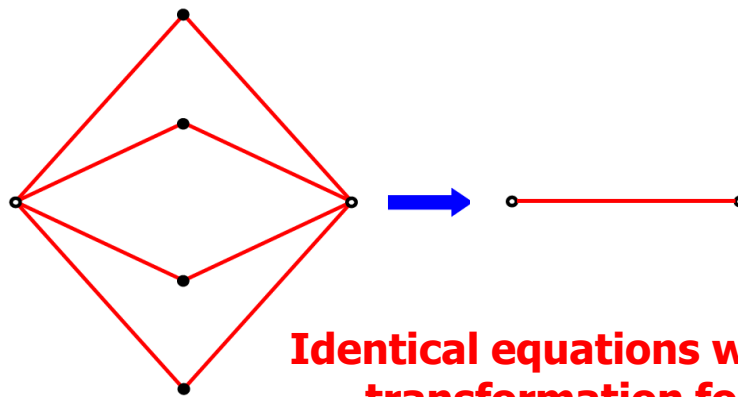


Construction of a Hierarchical Lattice (d=3)

Length rescaling factor, $b = 2$
Volume rescaling factor, $b^d = 8$



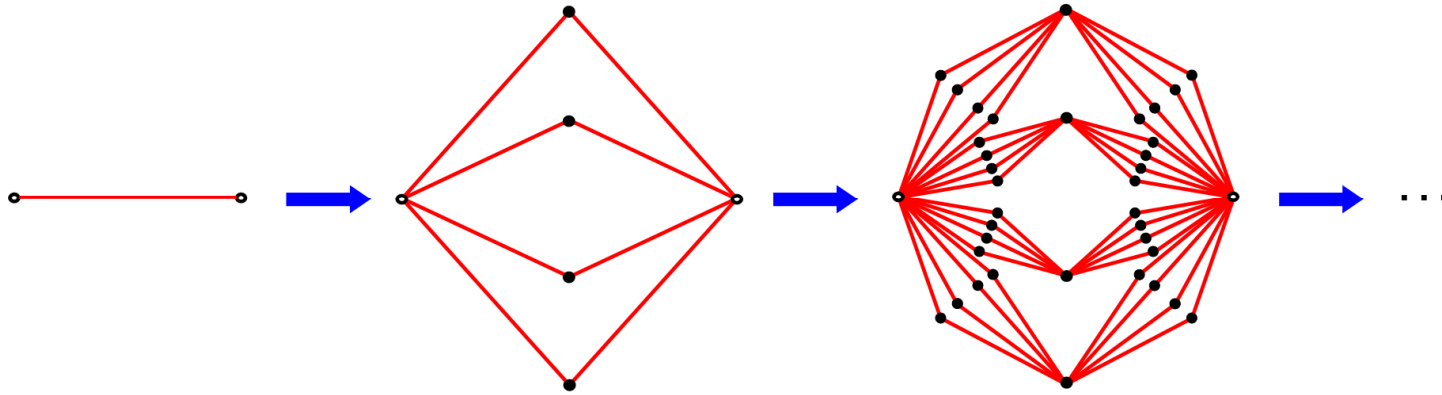
Renormalization-Group Transformation for this Hierarchical Lattice (exact)



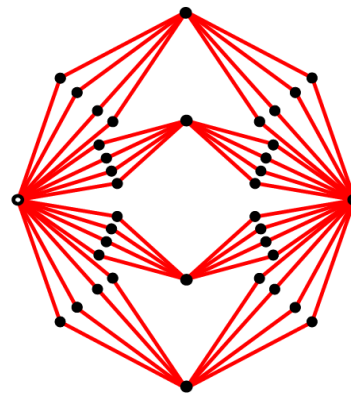
Identical equations with the approximate transformation for the cubic lattice

Construction of a Hierarchical Lattice (d=3)

Length rescaling factor, $b = 2$
Volume rescaling factor, $b^d = 8$

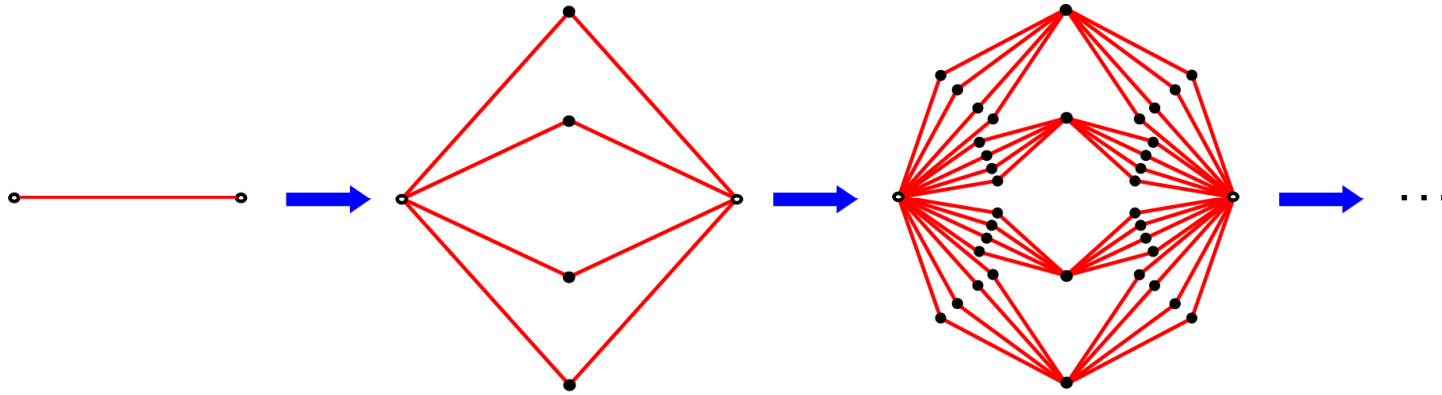


Renormalization-Group Transformation for this Hierarchical Lattice (exact)

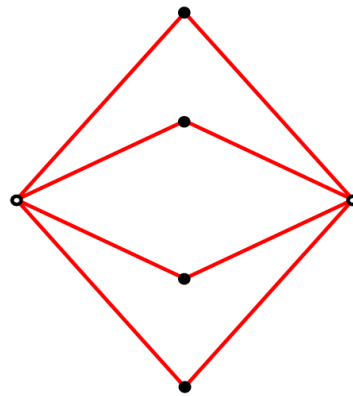


Construction of a Hierarchical Lattice (d=3)

Length rescaling factor, $b = 2$
Volume rescaling factor, $b^d = 8$

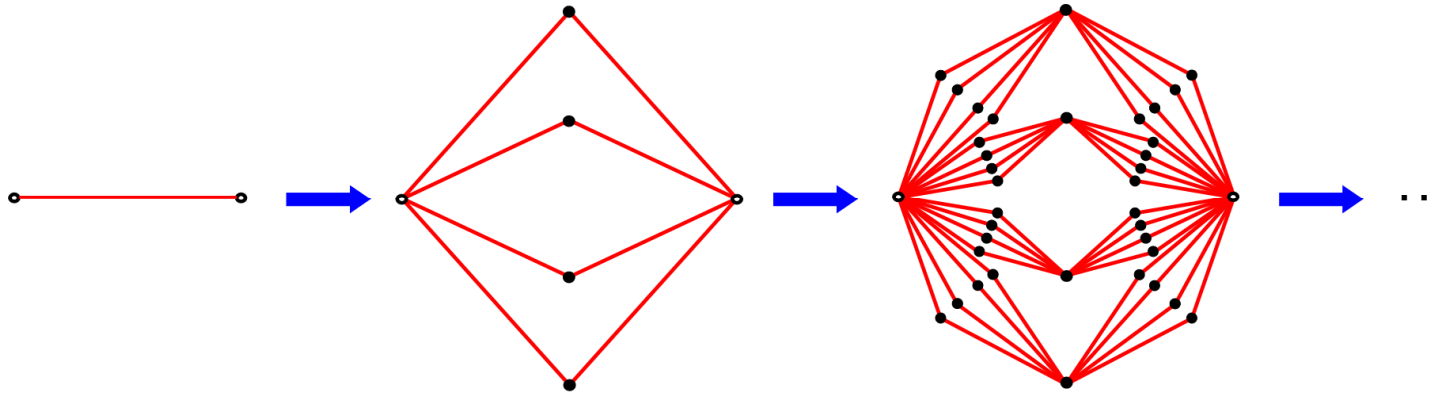


Renormalization-Group Transformation for this Hierarchical Lattice (exact)



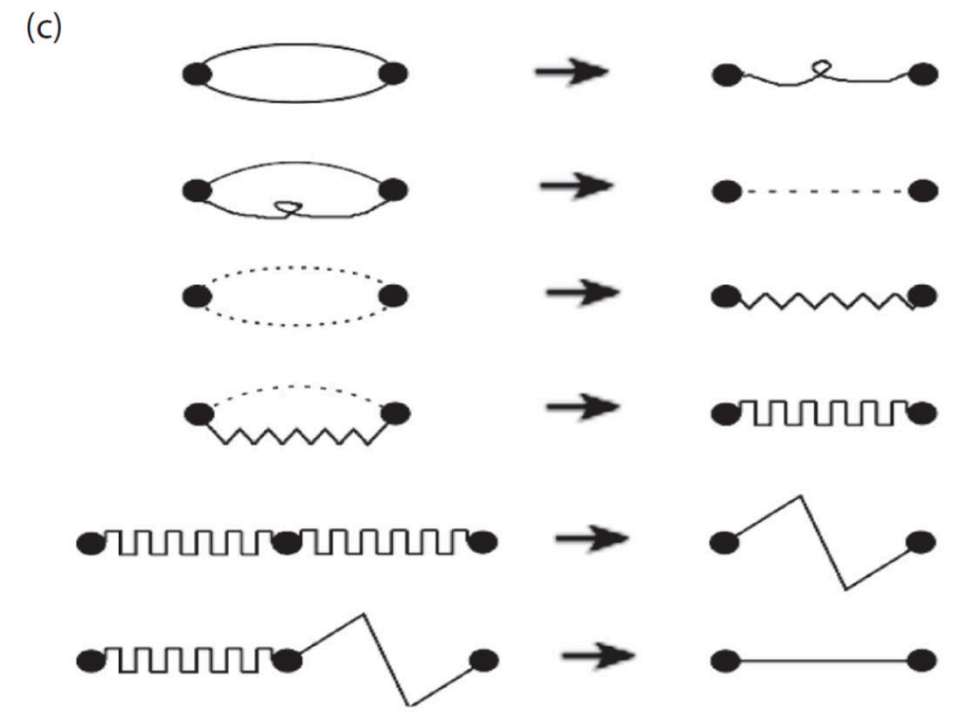
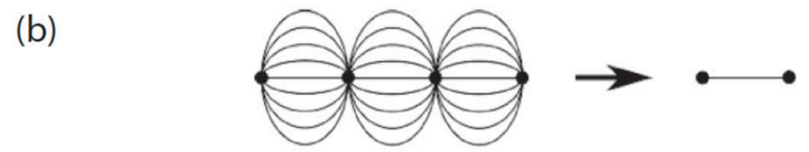
Construction of a Hierarchical Lattice (d=3)

Length rescaling factor, $b = 2$
Volume rescaling factor, $b^d = 8$



**Renormalization-Group Transformation for this Hierarchical Lattice
(exact)**





Incommensurate and commensurate phases in asymmetric clock models

S. Ostlund

Laboratory of Atomic and Solid State Physics, Clark Hall, Cornell University, Ithaca, New York 14853

(Received 15 December 1980)

When the ordinary nearest-neighbor p -state clock model (discrete xy model) is generalized to include asymmetric interactions, an incommensurate phase appears for integer $p \geq 3$ in addition to the usual liquid and commensurate phases. Aside from being theoretically interesting, it is of practical importance in studies of the commensurate-incommensurate transition where the existence of a discrete nearest-neighbor model with this property gives a computational advantage over further-neighbor and continuum models. For $p = 3$, the incommensurate phase always has a high degree of discommensuration and a Lifshitz point will occur where the incommensurate, liquid, and commensurate phases coincide. For $p = 2$ no incommensurate phase occurs. The system is analyzed at low temperature using a transfer matrix technique recently used by J. Villain and P. Bak to analyze a similar model with further-neighbor interactions.

Commensurate-Incommensurate Phase Diagrams for Overlayers from a Helical Potts Model

M. Kardar and A. Nihat Berker

Department of Physics, Massachusetts Institute of Technology, Cambridge, Massachusetts 02139

(Received 22 March 1982)

Oversaturated layers such as krypton on graphite are represented by a triplet helical Potts model, incorporating domain walls and antiwalls, and their crossings and annihilations (dislocations). Renormalization-group treatment yields a disordered phase between commensurate and incommensurate phases, down to zero temperature. Coadsorption produces a first-order transition directly between the commensurate and incommensurate phases, in analogy to temper embrittlement.

Domain Walls and the Melting of Commensurate Surface Phases

David A. Huse and Michael E. Fisher

Baker Laboratory, Cornell University, Ithaca, New York 14853

(Received 22 July 1982)

Commensurate adsorbed surface phases, particularly $p \times 1$ rectangular and $\sqrt{3} \times \sqrt{3}$ hexagonal phases, exhibit two (or more) classes of domain wall, reflecting a lower than ideal symmetry; these compete statistically and undergo wetting transitions. Scaling arguments and model calculations indicate that new types of continuous melting transitions, possibly already seen in Kr on graphite, can thereby arise.

Potts-like behavior should be maintained along the critical line, at least for a range of ζ near ζ_0 . Nevertheless, as in Fig. 2(b), a tricritical point, T_3 , and first-order segment may appear and, possibly, also a new multicritical point, M , and a *subsequent* chiral transition region.⁸ We believe that phase diagrams like Fig. 2 can be realized in physical systems. To distinguish the possibilities we present, first, a scaling argument, applicable to the disordered, melted phase, which suggests that chiral melting may already have been seen in Kr on graphite³; second, we discuss calculations for a *uniaxial chiral Potts* or *asymmetric $p=3$ clock model*,^{5,9} which indicate an isolated Potts multicritical point and a new chiral transition.

the commensurate phase, and ν . At a continuous commensurate-incommensurate transition \bar{q} and $\bar{\beta}$ are well defined in the incommensurate, floating solid^{4,11} although κ_x and ν are not; but scaling implies $\bar{\beta} = \nu'$, generally.

The symmetric p -state coupling quoted above is generalized in the uniaxial chiral (or asymmetric) clock models^{5,9} to $-J \cos[2\pi(n_i - n_j + \vec{\Delta} \cdot \hat{R}_{ij})/p]$, where \hat{R}_{ij} is a nearest-neighbor vector. Then for a small chiral field, $\vec{\Delta} = \hat{x}\Delta$, like pairs, 00, 11, ..., are still preferred to unlike pairs *but*, along the x axis, the + pairs, 01, 12, ..., are favored over the - pairs, 10, 21, ..., when $\Delta > 0$; likewise, as has been confirmed by low-temperature expansions, there are two distinct wall tensions, which satisfy $\Sigma_+ < \Sigma_-$ for $\Delta > 0$. On a square lattice